

Irradiation models for ULXs and fits to optical data

Christopher Copperwheat¹, Mark Cropper¹ Roberto Soria^{1,2} and Kinwah Wu¹

¹ Mullard Space Science Laboratory, University College London, Holmbury St. Mary, Dorking, Surrey, RH5 6NT, UK

² Harvard-Smithsonian Center for Astrophysics, 60 Garden Street, Cambridge, MA 02138, USA

Received:

ABSTRACT

We have constructed a model which describes the optical emission from ultra-luminous X-ray sources (ULXs), and have used it to constrain the parameters of seven ULX systems. Our model assumes a binary nature for ULXs, and accounts for optical emission from an X-ray irradiated companion star and accretion disk. We apply our model to six different ULX optical counterparts observed with *HST*, and one observed with the ESO VLT, and determine the mass, radius and age of the donor stars in these systems. In addition, we obtained constraints for the black hole (BH) mass in some cases. We use the mass accretion rate implied by the X-ray luminosity of these sources as an additional constraint on the donor star, by assuming the mass transfer is driven by the stellar nuclear evolution. We find that in general the donors are older and less massive than previously thought, and are consistent with being of spectral type B. We discuss how these results affect our understanding of the evolution and history of ULXs. Where we can constrain the BH masses, we find them to be consistent with stellar mass BHs or intermediate mass BHs of order $\sim 100M_{\odot}$. We make predictions for future observations of optical/infrared ULX counterparts, calculating binary periods for different BH masses in each of the seven sources.

Key words: black hole physics — X-rays: galaxies — X-rays: stars — accretion, accretion discs

1 INTRODUCTION

Ultraluminous X-ray Sources (ULXs) are point-like, non-nuclear X-ray sources which have inferred X-ray luminosities in excess of 10^{39}erg s^{-1} , assuming that the emission is isotropic. Some sources have X-ray luminosities even greater than 10^{40}erg s^{-1} , which is far in excess of the Eddington limit for a stellar mass black hole (BH) with mass $3\text{--}20M_{\odot}$. ULXs have been observed in many nearby galaxies (Fabbiano & White 2003; Swartz et al. 2004; Liu & Bregman 2005), implying that they are populous. To explain the large inferred isotropic luminosities of these sources, it has been proposed that the accreting object is a black hole of mass $50\text{--}10000M_{\odot}$ – an intermediate mass black hole (IMBH) (Colbert & Mushotzky 1999; Makishima et al. 2000). Such a mass range fits between those of the two well-known populations: the stellar mass BHs commonly found in our galaxy and the supermassive BHs in active galactic nuclei. The existence of IMBHs has important consequences for the theories of BH formation and evolution. It is still a mystery how supermassive BHs were formed. A continuous BH mass spectrum would suggest an evolutionary link between the three classes, thus allowing us to better understand BH formation in the younger universe.

Whether IMBHs exist or not is currently under intense

debate. The emission from ULXs may not be isotropic. If the emission is collimated or relativistically beamed (King et al. 2001; Körding, Falcke & Markoff 2002; Fabrika 2004), the accretion rates of the systems do not need to violate the Eddington limit. However, there is evidence that some sources are truly ultraluminous (Fabbiano 2004). An example is the ULXs associated with extended, diffuse H α nebulae, which are more naturally explained by models with isotropic illumination of the interstellar medium by a central X-ray source (Pakull & Mirioni 2002; Miller et al. 2003). Low-frequency quasi-periodic oscillations (QPOs) in the X-ray emission from some sources (M82 X-1: Strohmayer & Mushotzky 2003; Holmberg IX X-1: Dewangan, Griffiths & Rao 2006; NGC 5408 X-1: Strohmayer et al. 2007) suggest non-beamed emission and hence a truly high luminosity for those sources. Low-frequency breaks in the power density spectra of NGC4559 X-7 (Cropper et al. 2004) and NGC5408 X-1 (Soria et al. 2004) are also consistent with accretors more massive than galactic BHs. However, population studies based on the luminosity function of ULXs suggest a more modest upper limit on the mass of IMBHs than previously thought. The break in the luminosity function at $\sim 2.5 \times 10^{40}\text{erg s}^{-1}$ (Swartz et al. 2004; Gilfanov, Grimm & Sunyaev 2004) sug-

gests the bulk of the IMBH population lies below $\sim 150M_{\odot}$, assuming accretion at the Eddington limit.

Another argument proposed for IMBH accretors is based on the detection of a spectral component interpreted as emission from a cool accretion disk (Miller et al. 2004). However, this spectral argument has been disputed (e.g., Stobbart, Roberts & Wilms 2006; Gonçalves & Soria 2006). Alternative spectral models based on high-temperature, super-Eddington disks have been proposed (Stobbart et al. 2006; Ebisawa et al. 2003). It has also been suggested that super-Eddington accretion can occur in BH systems through a thin disk covered by a Comptonizing corona (Socrates & Davis 2005; Done & Kubota 2005). An accretion disc dominated by radiation pressure may exhibit strong density clumping. If the density inhomogeneities are on length scales much smaller than the disc scale height, such clumpy accretion discs could permit the radiation luminosity to exceed L_{Edd} by factors of $\sim 10 - 100$ (Begelman 2002).

Since the X-ray data alone can be interpreted in different ways, we have sought an alternative channel to X-ray investigations by which the nature of ULXs can be elucidated. The ULX may contain a stellar mass BH with super-Eddington accretion or an IMBH. The optical/infrared (optical/IR) properties of ULXs will be strongly affected by the intense X-ray radiation field heating the donor star and accretion disk. The emission from the heated star may be the dominant optical component (as in the case of high mass X-ray binaries). Alternatively, theoretical modelling has shown that the heated accretion disc might dominate (Rappaport, Podsiadlowski & Pfahl 2005; Copperwheat et al. 2005), analogous to low mass X-ray binaries. In Copperwheat et al. (2005) we considered such a binary model for ULX and derived a formulation which calculated the intensity and colour variations from the intrinsic and re-radiated emission as a function of several parameters such as X-ray spectral hardness, black hole mass and inclination. The predictions of the calculations can be used to identify the optical counterpart, to determine the intrinsic properties of the component stars, and to determine the relative contributions of the star and disk. We may also use the optical/IR emission as a diagnostic of the X-ray emission and the accretion processes in ULXs/IMBHs.

In recent times, there have been a number of optical observations of ULXs with the Hubble Space Telescope (*HST*) and ground based 8-m class telescopes. These observations have resulted in the isolation of optical counterparts of some ULXs, and have provided colours and magnitudes in the optical wavebands (see, e.g. Kaaret, Ward & Zezas 2004; Liu, Bregman & Seitzer 2004; Kuntz et al. 2005). In this paper, we apply our model to determine the properties of the ULX counterparts observed by these telescopes.

In Section 2 we briefly reprise the Copperwheat et al. (2005) model and describe the recent refinements. In Section 3 we apply our model to seven ULX sources. In Section 4 we discuss the implication of our results on the current views regarding the nature of ULXs and IMBHs.

2 MODEL

2.1 Irradiation in ULX binaries

The Copperwheat et al. (2005) model assumes a binary system with a BH accreting matter from a companion star. We assume the X-ray emission from the ULX is isotropic. Our model considers the effects of radiative transport and radiative equilibrium in the irradiated surfaces of both the star and an accretion disc, using the prescription described in Wu et al. (2001).

We assume the disc is geometrically thin, and for the star we include both gravity and limb darkening effects, and the effects of radiation pressure. We assume the companion star is filling its Roche lobe and the BH is accreting matter via Roche lobe overflow. This provides a geometrical constraint on the system that is key in our determination of the optical luminosity of both the star and the disc. These assumptions are valid when the X-ray luminosity is in excess of 10^{40}erg s^{-1} , since the donor star cannot generate a sufficient stellar wind in order to maintain the accretion rate required by this X-ray luminosity. However, some of the sources we detail in this section have X-ray luminosities of the order of 10^{39}erg s^{-1} . At this point it is conceivable that the accretion mechanism could be a wind from a massive supergiant. In this case we cannot constrain the binary separation without temporal observations that reveal the binary period, which means we cannot quantify the stellar irradiation. However, a wind-fed BH would only intercept a few percent of the stellar wind from a star, and so given the mass accretion rate of $\sim 10^{-7}M_{\odot}/\text{yr}$ necessary to provide the observed X-ray luminosity, a wind loss of $\sim 10^{-5}M_{\odot}/\text{yr}$ would be required from the star, which is very high. ULXs also tend to have lower column densities than the typical wind-fed sources observed in the Galaxy/LMC (Stobbart et al. 2006). We therefore consider Roche lobe overflow as the accretion mechanism to be a reasonable assumption for all of the sources down to 10^{39}erg s^{-1} .

Copperwheat et al. (2005) showed that the results of the irradiative calculations could depend sensitively on the assumed hardness of the X-rays, which is specified by a parameter ξ , where $\xi = S_h/S_s$ and S_h and S_s are the hard and soft components of the X-ray flux respectively. As in Copperwheat et al. (2005), the absorption coefficients of the soft and hard X-rays are $k_s\kappa$ and $k_h\kappa$, where κ is the absorption coefficient of the optical radiation and $k_s > 1$ and $k_h < 1$ defines our soft/hard X-ray convention. The band boundary is a parameter to be determined. In Copperwheat et al. (2005) we found that if we set $k_s = 2.5$ and $k_h = 0.01$, then for an input spectrum consisting of a blackbody and power-law component, this results in a soft/hard band boundary of 1.5keV.

Determining the hardness ratio of the incident X-rays on the accretion disk is not straightforward and is complicated by the presence of absorption. Absorption tends to harden the X-rays. If the absorbing region which produces this hardened spectrum is intrinsic to the X-ray emitting region itself, the disk and star will be irradiated by the same hard X-ray spectrum that we observe. If the absorbing region is located between the binary system and the observer, then the irradiating X-rays will be much softer than is observed.

By examining X-ray observations from ULX X-7 in

NGC 4559 (Copperwheat et al. 2004) we see that for this source, reasonable physical values for the hardness ratio range from $\xi \sim 0.1$ to ~ 1 . In this paper, we set the hardness ratio to 0.1 since we expect a locally soft irradiating spectrum. In Section 4.6 we examine how varying this parameter affects our results.

In order to determine the mass accretion rates and irradiating flux for each source, we use the characteristic average values of X-ray luminosity as given by the authors listed in Table 1. We note that this may be a source of uncertainty in our results: since the X-ray observations are not contemporary with the optical observations, the X-ray luminosity and spectrum at the time of the optical observation may be different.

We assume the compact object in the binary system is a BH, but we do not assume it to be an IMBH. For all sources we use BH masses of $10 - 1000M_{\odot}$ in our model, a range that encompasses both a stellar mass and an intermediate mass nature for the BH. We do not use BH masses of beyond $1000M_{\odot}$ since at this point the optical emission is dominated by a large disc, and increasing the BH mass further has little additional effect on our model results. Similarly, results for a BH mass of $10M_{\odot}$ can be taken to apply to BHs with masses less than this.

2.2 Inclusion of stellar evolution models

As well as detailing our model in Copperwheat et al. (2005), we applied it to the candidates for the optical counterpart of ULX X-7 in NGC 4559. We took the masses, radii and luminosities of various main sequence (MS) and supergiant stars from the tables in Allen (1973). We included these parameters in our model, and hence were able to calculate the optical luminosity of the ULX if the companion star in the binary system was described by those parameters. We plotted tracks on colour magnitude diagrams, which describe the effect on the optical luminosity when the BH mass was varied. We compared these tracks to the measured colours and V band magnitudes of the candidates. This allowed us to constrain the properties of possible candidates.

In this paper we have further developed our method by using the Geneva stellar evolution models of Lejeune & Schaerer (2001) to provide more realistic stellar parameters, and also to provide constraints on the derived ages. We primarily use the high mass-loss tracks which are recommended for use when dealing with massive stars (Maeder & Meynet 1994). These extend up to a stellar age of $10^{7.5}$ yr. We supplement these with the standard tracks when we wish to consider less massive stars with an age greater than this. We input the set of stellar parameters at each point along the evolutionary tracks into our model. We use our model to produce colours and magnitudes appropriate for the irradiated star and disc. We do this for all relevant tracks, which enables us to include stellar age as an additional parameter in our analysis. We repeat this process as we vary the other important parameters, such as X-ray luminosity, the inclination and orientation of the binary system, and BH mass. We described the parameter space relatively completely in Copperwheat et al. (2005).

An additional parameter, introduced by our use of the Geneva tracks, is the stellar metallicity. We use a sub-solar ($Z = 0.2Z_{\odot}$) metallicity throughout. This is appropriate

given that many ULXs are in low-metal environments such as dwarf galaxies. Low-metal stars also lose less mass in stellar winds (Eldridge & Vink 2006). Therefore, we speculate that they may end their lives with bigger cores, which can more easily collapse directly into BHs (Heger et al. 2003).

We note that we assume the Geneva models and metallicity to be correct, so we have not taken into account any systematic error introduced by a difference between the stellar evolution as described by those models, and the evolution of a donor in a ULX binary system. A binary evolution code is not necessarily more appropriate, since we do not know when the binary evolved to a semi-detached state, and so we do not know to what extent the normal evolution of the star has been disrupted by the mass transfer. We therefore use a single-star model in this paper to describe the simplest case, where the donor star has not been significantly perturbed by the mass transfer.

2.3 Mass accretion rate as a constraint of the system parameters

For some of the sources in our analysis optical data alone is sufficient to determine the parameters of the donor star with good accuracy. For the others there is a large uncertainty even in establishing the luminosity class of the donor star, because the data can be fitted by a wide range of stellar parameters. In this situation, we can use addition conditions to constrain the parameter space.

We consider a method that makes use of the information provided by the X-ray data and model stellar evolutionary calculations, which is essentially independent of the optical/IR photometric observations. The X-ray luminosity L_x of an accreting object is given by the relation

$$L_x = \eta \dot{M} c^2, \quad (1)$$

where \dot{M} is the mass accretion rate and η is the efficiency parameter. For accretion onto BH, we may take $\eta = 0.1$, which is sufficient for the purpose of this study. A ULX luminosity of 10^{40} erg s $^{-1}$ therefore corresponds to a mass loss rate of $\dot{M} \simeq 1.8 \times 10^{-6} M_{\odot}$ yr for the donor star, if we assume all mass outflow from the star will be accreted onto the BH.

We suppose that mass transfer occurs due to the donor star overfilling its Roche-lobe, and the transfer is driven by a gradual volume expansion of the star as it evolves away from its main-sequence phase. For a quasi-steady state, the rate of mass loss from the donor star \dot{M}_2 is given by

$$\dot{M}_2 = \frac{M_2}{\zeta_{2s} - \zeta_{2r}} \left[\frac{2}{\tau_J} - \frac{1}{\tau_{th}} - \frac{1}{\tau_{nuc}} \right], \quad (2)$$

where M_2 is the mass of the donor star, ζ_{2s} and ζ_{2r} are the adiabatic indices of the mass donor star and its Roche lobe respectively, τ_J is the time scale of orbital angular momentum loss, τ_{th} is the thermal time scale of the donor star and τ_{nuc} is the nuclear evolutionary time scale of the donor star (Ritter 1988; D'Antona, Mazzitelli & Ritter 1989). Stable mass transfer occurs when $\zeta_{2s} - \zeta_{2r} > 0$.

The orbital evolution of binary undergoing mass transfer is governed by the following equation (see Wu 1997):

$$\frac{\dot{a}}{a} = 2 \frac{\dot{J}}{J} - 2 \frac{\dot{M}_2}{M_2} \left[1 - \frac{\beta}{q} - \frac{1}{2} \left(\frac{1-\beta}{1+q} \right) - \frac{\alpha}{q} (1-\beta)(1+q) \right], \quad (3)$$

where a is the orbital separation, J is the orbital angular momentum, q is the mass ratio M_1/M_2 , β is the fraction of mass loss from the donor star accreted onto the BH, α is the specific angular momentum carried away by mass loss from the system, and “dot” denotes the time derivative. For conservative mass transfer, which is assumed in this study, we have $\dot{J} = \alpha = 0$, and $\beta = 1$. It follows that

$$\frac{\dot{a}}{a} = -2\left(\frac{q-1}{q}\right)\frac{\dot{M}_2}{M_2}. \quad (4)$$

The Roche-lobe radius R_L of the donor star and the orbital separation a is well approximated via

$$\frac{R_L}{a} = \frac{0.49q^{-2/3}}{0.6q^{-2/3} + \ln(1 + q^{-1/3})} \quad (5)$$

(Eggleton 1983). The Roche-lobe filling condition requires $R_L = R$, where R is the radius of the donor star. Suppose that the mass transfer is quasi-steady, *i.e.* $\dot{R}_L = \dot{R}$. By combining these conditions with Equations 4 and 5, we obtain

$$\frac{\dot{M}_2}{M_2} = \frac{\dot{R}}{R} \left[\frac{q}{2(1-q) + (1+q)[2/3 - g(q)]} \right], \quad (6)$$

where the function $g(q)$ is given by

$$g(q) = \frac{(2/5)q^{-2/3} + q^{-1/3} [3(1 + q^{-1/3})]^{-1}}{(3/5)q^{-2/3} + \ln(1 + q^{-1/3})}. \quad (7)$$

For mass transfer driven by nuclear evolution,

$$\dot{M}_2 \approx -\gamma \frac{M_2}{\tau_{nuc}}, \quad (8)$$

where γ is a positive, slowly varying parameter depending on the spectral type and mass of the donor star and the orbital parameters. The faster the donor star evolves, the higher the mass transfer rate will be, and how rapid mass transfer occurs is dictated by the evolutionary timescale. The rate of expansion of the stellar radius \dot{R} and hence the mass accretion rate \dot{M} at particular evolutionary stage of the donor star can be derived from stellar evolutionary tracks.

Unless stated otherwise, we set the the mass accretion rate for sources with X-ray luminosities $L_x \sim 10^{40} \text{ erg s}^{-1}$ to be $\sim 10^{-6} M_\odot/\text{yr}$ and other sources with $L_x \sim 10^{39} \text{ erg s}^{-1}$ to be $\sim 10^{-7} M_\odot/\text{yr}$.

2.4 Mass transfer timescale considerations

Some of the models constructed to support stellar-mass BHs in ULXs propose they are intermediate- or high-mass X-ray binaries undergoing a phase of mass transfer on thermal timescales (King et al. 2001; King 2002).

Thermal-timescale mass transfer can occur when the ratio q of donor mass to BH mass exceeds a critical value $q_{crit} \sim 1$. The mass transfer is initiated by orbital evolution of the binary or nuclear evolution of the star, and for mass ratio of $q > q_{crit}$ the Roche lobe of the secondary will shrink in response to the transfer. This will result in more of the donor spilling out of the Roche equipotential and a phase of rapid mass transfer. In response to the mass loss, the donor will decrease in size. In general, we find that the thermal timescale is much shorter than the nuclear evolutionary timescale for early type stars. On the other hand, relatively massive donors are required to achieve $q > q_{crit}$. If

a large fraction of ULXs are found to be undergoing thermal-timescale mass transfer then the parameter space is much smaller than we examine, since the runaway scenario can only occur with a mass ratio $q > q_{crit}$.

In Equation 8 we take the mass transfer to be proceeding on the nuclear evolutionary timescale; thus we do not consider thermal-timescale transfer in this paper explicitly. Our model breaks down when the thermal timescale is comparable to the nuclear evolutionary timescale of the donor. In this case the star cannot adjust to the mass loss fast enough to prevent runaway, unstable mass transfer. Then the outer layers of the star cannot remain in radiative equilibrium and the assumptions of our model are violated.

Note from Equation 2 that our formalism is versatile enough to consider thermal timescale mass transfer (in this case the mass transfer rate cannot be deduced directly from the stellar evolutionary track). Our irradiation model is applicable irrespective of the mechanism and timescale of mass transfer.

2.5 Inclination and orientation considerations

For all ULXs the inclination with respect to the observer is currently unknown. At one extreme, the orbital plane of a binary is perpendicular to the plane of the sky ($\cos(i) = 0.0$). In this case with a thin disk, all of the optical flux we observe will be from the star. For any other inclination the optical flux will also contain a disc component, the relative contribution of which will increase as $\cos(i)$ is increased to 1.0. The phase of the companion star at the time when the observations were made is also unknown. If the star is in superior conjunction with respect to the observer, the observation will be of the irradiated hemisphere of the star. If the star and the observer are in inferior conjunction, the observation will be of the hemisphere facing away from the BH and therefore the flux from the star will contain little or no irradiated component.

We noted in Copperwheat et al. (2005) that the geometric constraints of the binary system determined whether reprocessed light from the disc or the star dominated the optical/IR emission. The disc is truncated by tidal forces, and so when the separation between the star and the BH is large, the disc is also large and hence more likely to be the dominant optical component. A large separation is a consequence of assuming a high BH mass, so a high BH mass implies disc dominated optical/IR emission. We would expect that inclination would therefore dominate the geometrical effects in high BH mass systems. A low BH mass generally implies the emission is dominated by the donor star. We would therefore expect the phase of the star to have a significant effect on the results only in the cases where we assume a low BH mass.

We concentrate our analysis on the general case where there is an irradiated component from both the star and the disc. We therefore start by assuming $\cos(i) = 0.5$. As we demonstrated in Copperwheat et al. (2005) this orientation already results in a strong contribution to the optical flux from the disc, and increasing the inclination to $\cos(i) = 1.0$ has little additional effect. By considering the cases where the star is in superior and inferior conjunction we examine the phases where the stellar contribution to the observed optical emission is strongest and weakest for this inclina-

tion. We then additionally consider superior conjunction and $\cos(i) = 0.0$, describing the case when all of the optical flux is from the irradiated hemisphere of the star. When we assume inferior conjunction and take $\cos(i) = 0.0$, we would see only the unirradiated hemisphere of the star. In this case it would be appropriate to use a standard unirradiated star. These extreme states allow us to explore relatively completely the inclination and phase orientation parameter space.

3 APPLICATION TO OBSERVATIONS

We now apply our calculations to the observed optical counterparts of six ULXs observed with *HST*, and one observed with the ESO VLT telescope. The photometric values we have used are in Table 1. Where necessary, we have converted the values to absolute magnitudes using the distances given in the table.

We have corrected the values for the NGC 4559 and the NGC 1313 ULXs using the Galactic $E(B-V)$ values given in Soria et al. (2005) and Mucciarelli et al. (2005) respectively, and $A_V/E(B-V) = 3.1$. For the M101 ULX we use the $E(B-V)$ from Kuntz et al. (2005), which includes Galactic reddening and reddening from the disk of M101. In the case of the NGC 5204 ULX, we follow Liu, Bregman & Seitzer (2002) for the reddening correction, using $n_H = 10^{21} \text{ cm}^{-2}$ and assume the Galactic relation $n_H = 5.8 \times 10^{21} E(B-V)$ (Bohlin, Savage & Drake 1978). The remaining objects were already corrected for Galactic reddening.

We determine the uncertainty in the values given in Table 1 by taking the error given for the original photometric values, and combine this with any additional uncertainty we have introduced by correcting for reddening. We base our confidence intervals on these errors, and fix the X-ray luminosity and hardness. We assume the distances given in Table 1 to be correct, and so do not introduce any additional uncertainty where we have converted from apparent to absolute magnitudes.

For each source, we take each evolutionary track in turn, and comparing the available photometric observations with our model calculations, calculate the variation in the χ^2 -squared statistic along it. We then combine our tracks, and determine the range of the important parameters to 68%, 90%, 95% and 99% confidence levels. The results of our calculations are in Figures 3 to 11 and Tables 2 to 5. We show all four confidence levels in the figures, but the values we quote in the tables and the text are taken at the 90% confidence level.

3.1 ULX X-7 in NGC 4559

Soria et al. (2005) used *HST* WFPC2 observations to study the optical environment of ULX X-7 in NGC 4559, a source with an average X-ray luminosity of $10^{40} \text{ erg s}^{-1}$ (Cropper et al. 2004). They found eight possible candidates for the ULX optical counterpart, listing the B , V and I_C standard magnitudes for each in table 2 of that paper.

We applied our model to this source in Copperwheat et al. (2005). We now do this again, using the revised model as described in Section 2. We apply the extinction correction for absorption within our galaxy given in Soria et al. (2005) to the photometric observations.

As in Copperwheat et al. (2005), we find that candidates 2, 3 and 4 are consistent with our model only when we use a BH mass of $\simeq 1000 M_\odot$ and an inclination of $\cos(i) = 0.0$.

Soria et al. (2005) suggested that candidate 1 was the most likely counterpart. The findings of Copperwheat et al. (2005) are consistent with this and so for our further analysis of this source we will assume candidate 1 is the optical counterpart.

In Figures 1 and 2 we plot the confidence contours for the stellar age, mass and radius against the BH mass, for an inclination of $\cos(i) = 0.5$ in Figure 1 and $\cos(i) = 0.0$ in Figure 2. We assume the star is in superior conjunction in both cases.

We see first that there is an upper bound on the BH mass of $\sim 35 M_\odot$ in the $\cos(i) = 0.0$ case. As for the donor star parameters, if we examine the $\cos(i) = 0.5$ case first we see that the age ranges from $10^7 - 10^8 \text{ yr}$, the mass ranges from $5 - 20 M_\odot$ and the radius is between 9 and $30 R_\odot$, with the lower radii implying a higher BH mass. For the $\cos(i) = 0.0$ case the age and mass range is similar. The radius lies between 51 and $72 R_\odot$ when we assume this inclination.

These values are consistent with candidate 1 being of a similar mass and age to the other candidates within the error circle (Soria et al. 2005), with its increased luminosity due to the effects of irradiative heating.

3.2 ULX X-6 in M81

This source has an average X-ray luminosity of $2 \times 10^{39} \text{ erg s}^{-1}$ (Roberts & Warwick 2000). Liu et al. (2002) found an optical counterpart they considered unique to this ULX (designated NGC 3031 X-11 in that paper), and reported B , V and I magnitudes derived from *HST* ACS observations (Table 1).

We first examine the case where this source is at superior conjunction and $\cos(i) = 0.5$. We find that for this orientation our model is a poor fit to the observation at the 90% confidence level: the irradiated disk/star are together too luminous to match the observation for any combination of star and BH. We therefore chose to adjust the hardness ratio of the irradiating X-ray spectrum in this case in order to fit our model to the observation. When we lower ξ to 0.01, we find a good fit to the data. We show the confidence contours in Figure 3. We see that the stellar age ranges from $10^6 - 10^{8.7} \text{ yr}$, with a lower stellar age implying a higher BH mass. The stellar mass ranges from $1.5 - 14 M_\odot$, and the stellar radius ranges from $2.5 - 8 R_\odot$.

When we assume the star to be in inferior conjunction, we again require a reduced hardness ratio of $\xi = 0.01$ in order to obtain a good fit. We find that most of the parameter space that we found fitted with our model for the superior conjunction case is contained within that here. In addition, we find that for low BH masses we can fit larger stars of radius $10 - 17 R_\odot$ with the observation. These parameters represent cases where the majority of the optical emission is from the unirradiated hemisphere of the star. The small, but not insignificant disc contribution, as well as the Roche lobe shape of the star accounts for the difference between our fitted stellar parameters and those of Liu et al. (2002) in this inferior conjunction case. At higher BH masses the emission is disk dominated and our results are not dependent on the phase of the star.

Table 1. The photometric data we have used for the ULX in this work. Where necessary, we have converted the figures given in the references to absolute magnitudes and have applied reddening corrections for galactic absorption.

	M_B	M_V	M_{R_c}	M_{I_c}	Distance (Mpc)	
NGC 4559 X-7	-7.22 ± 0.19	-7.03 ± 0.16		-6.98 ± 0.16	10	(Soria et al. 2005)
M81 X-6	-4.28 ± 0.04	-4.18 ± 0.03		-4.20 ± 0.07	3.63	(Liu et al. 2002)
M101 ULX-1	-6.19 ± 0.15	-5.92 ± 0.12		-5.81 ± 0.16	7.2	(Kuntz et al. 2005)
NGC 5408 ULX	-6.4 ± 0.2	-6.4 ± 0.2		-6.1 ± 0.1	4.8	(<i>Subaru</i> and <i>HST</i> archival data)
Holmberg II ULX	-6.03 ± 0.19	-5.78 ± 0.11			3.05	(Kaaret et al. 2004)
NGC 1313 X-2 (C1)	-4.7 ± 0.18	-4.5 ± 0.18	-4.2 ± 0.18		3.7	(Mucciarelli et al. 2005)

	HSTMAG	F220W	F435W	F606W	F814W	Distance (Mpc)
NGC 5204 ULX		-8.51 ± 0.11	-6.49 ± 0.11	-5.44 ± 0.13	-4.38 ± 0.13	4.3 (Liu et al. 2004)

We examine next the case when $\cos(i) = 0.0$ (Figure 2). In this orientation, we can fit our model with the observation for a hardness ratio of $\xi = 0.1$. We note first of all that there is an upper bound on the BH mass of $33M_\odot$. The stellar age that fits with the observation ranges from $10^{7.9} - 10^{8.7}$ yr, and the mass and radius range from $3 - 5.5M_\odot$ and $10 - 15R_\odot$ respectively. These values fit equally well, when we set $\xi = 0.01$, since the stellar luminosity is much less sensitive to changes in the X-ray hardness than the disk.

Liu et al. (2002) found the field stars in the vicinity of this ULX range in age from $1.0 \times 10^6 - 1.0 \times 10^8$ yr. If we assume the donor in the ULX binary is of a similar age, we see from Figure 2 that the stellar parameters are very tightly constrained in the $\cos(i) = 0.0$ case. In the $\cos(i) = 0.5$ case (Figure 3), we see that there is a lower limit on the BH mass of $20M_\odot$ if we constrain the stellar age in this way.

3.3 ULX in NGC 5204

HST WFPC2 and ACS observations of the optical counterpart to a ULX in NGC 5204 were described in Liu et al. (2004). This source has an X-ray luminosity of $L_x \simeq 3 \times 10^{39}$ erg s $^{-1}$. We took the photometric measurements from Liu et al. (2004) and corrected those magnitudes for interstellar absorption using the N_H column density given in Liu et al. (2004).

We find our model is a very poor fit to the observation when we orient the system so as to include an irradiated disk and/or stellar component. This poor fit is caused by our constraint on the mass accretion rate. When we remove this constraint we find our model implies a companion star with a mass of 60 to $110M_\odot$, a radius of $13 - 15R_\odot$ and an age of $10^{6.3}$ yr or less. This is a young, massive star that is evolving rapidly in radius and is hence transferring mass at a high rate, so when we set an upper limit on the mass accretion rate as implied from the X-ray luminosity, this solution is precluded. The best solution with this constraint applied is for a BH mass of $1000M_\odot$ and a stellar age, mass and radius of $10^{5.3}$ yr, $52M_\odot$ and $9R_\odot$ respectively.

We note as an aside that, when we remove the constraint on the mass accretion rate, there is an upper bound on the BH mass of $240M_\odot$ when we assume an inclination of $\cos(i) = 0.5$.

3.4 M101 ULX-1

The source designated ULX-1 in M101 has a peak X-ray luminosity of $\simeq 1.2 \times 10^{39}$ erg s $^{-1}$. Kuntz et al. (2005) reported a unique optical counterpart and reported B, V and I magnitudes recorded with the *HST* ACS instrument. From these data, they deduced the companion star was a B type supergiant with a mass of 9 to $12M_\odot$. They also observed no significant variation in the optical magnitudes over a sixty day period.

When we use an inclination of $\cos(i) = 0.5$ we find a stellar age of $10^8 - 10^{8.7}$ yr, a mass of $2 - 7M_\odot$ and a radius of $6 - 30R_\odot$, with lower radius values implying a more massive BH.

As in the case of the ULX in NGC 5204, we find our model is a very poor fit to the observation when we use an inclination of $\cos(i) = 0.0$. Again, the poor fit is caused by the upper bound on the mass accretion rate – when we remove this constraint we find a star of age $10^{7.0}$ yr to $10^{7.3}$ yr, mass $11 - 100M_\odot$ and radius $12 - 33R_\odot$ fits the observation. These are much looser constraints on the stellar parameters than those reported by Kuntz et al. (2005). By allowing emission from both an irradiated star and disk component, the observation fits with a much wider range of binary systems.

3.5 ULX in NGC 5408

NGC 5408 contains a ULX with an X-ray luminosity of 10^{40} erg s $^{-1}$. This source was initially thought to be consistent with a beamed microquasar (Kaaret et al. 2003). More recent studies have shown disk emission and QPOs, which could be interpreted as evidence for an IMBH (Soria et al. 2004; Strohmayer et al. 2007). However, a soft disk component may also be explained by alternative scenarios that do not require an IMBH (Stobbart et al. 2006; Gonçalves & Soria 2006). Therefore, in this and other sources characterized by an X-ray soft excess, optical constraints on the system parameters can help break the degeneracy.

We use the archival *HST*/WFPC2 and *Subaru* observations to determine B, V and I photometric magnitudes for the optical counterpart. There are in fact a number of candidates for the optical counterpart within the *Chandra* error circle: we assume here the counterpart is the source which appears most luminous in the V-band *HST* observation.

We examine the $\cos(i) = 0.5$ case first (Figure 5). We see that we can fit a donor star of mass $6 - 24M_\odot$ to the

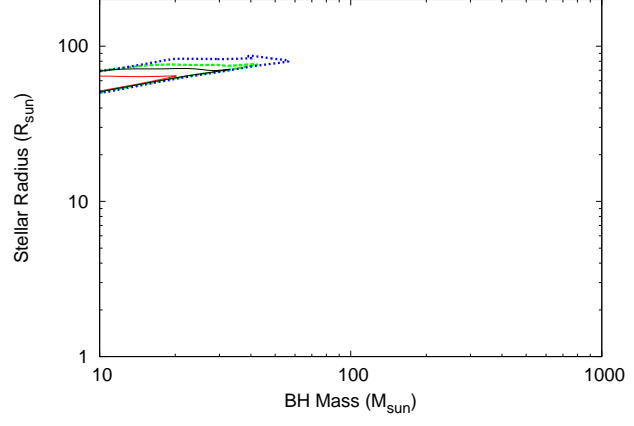
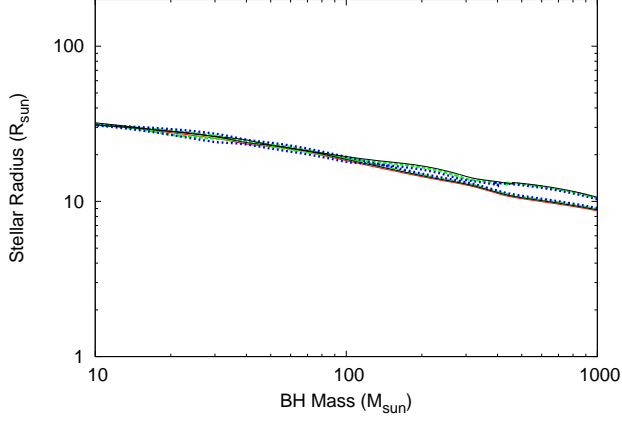
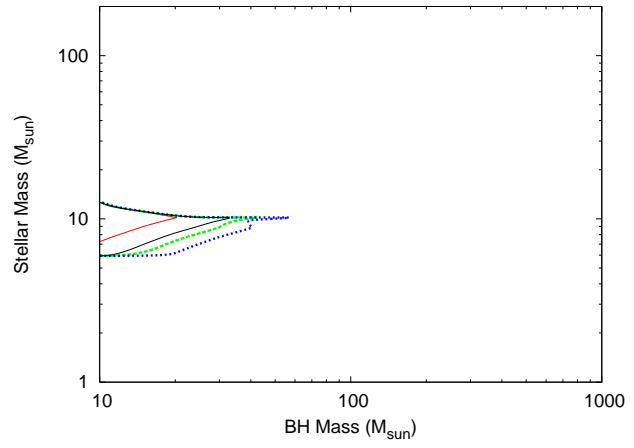
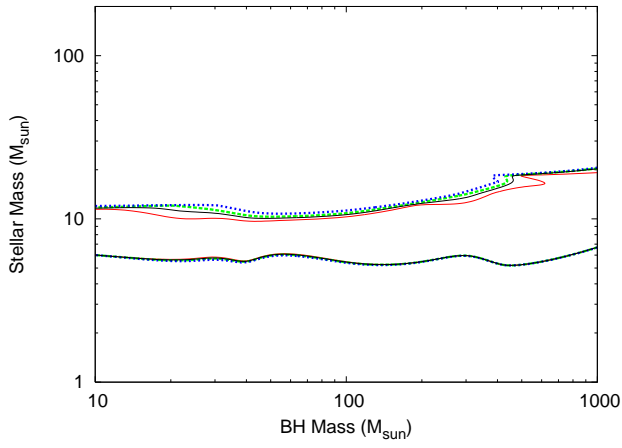
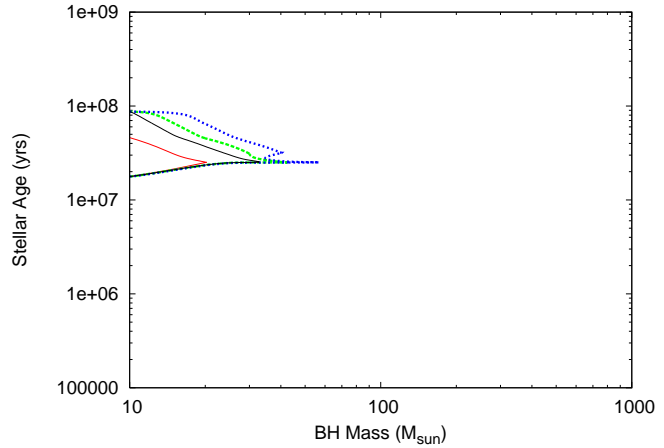
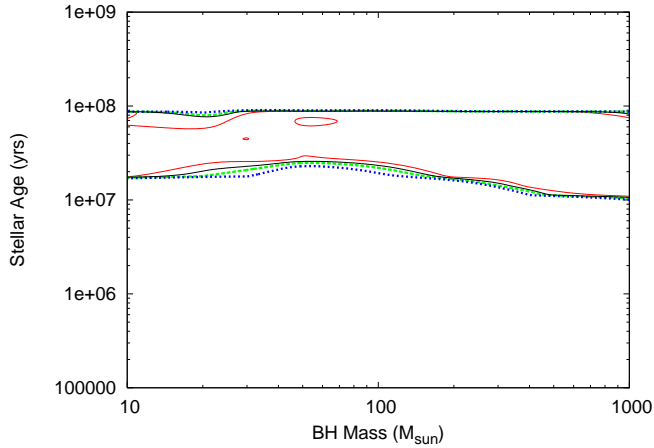


Figure 1. Confidence contours for the binary parameters for the source X-7 in NGC 4559, assuming candidate 1 is the optical counterpart. We assume a binary inclination of $\cos(i) = 0.5$, superior conjunction with respect to the observer and the star, and a stellar metallicity of $Z = 0.2Z_\odot$. We use an X-ray hardness ratio of $\xi = 0.1$. The red, black, green and blue lines denote the 68%, 90%, 95% and 99% confidence intervals respectively.

observational data over the entire BH mass range. These stars have ages of order 10^7 yr and radii of $23 - 44R_\odot$. We see also that when we assume a BH mass of greater than $100M_\odot$, we can fit more massive ($< 100M_\odot$), younger and more compact stars to the observation. A very massive ($>$

Figure 2. As for Figure 1, but with a binary inclination of $\cos(i) = 0.0$.

$67M_\odot$) donor is also possible when we use a BH mass of less than $30M_\odot$.

In the $\cos(i) = 0.0$ case, we see from Figure 6 that an upper bound of $110M_\odot$ exists. The donor star has an age of $10^7 - 10^{7.8}$ yr, a mass of $6 - 15M_\odot$ and a radius of $23 - 43R_\odot$.

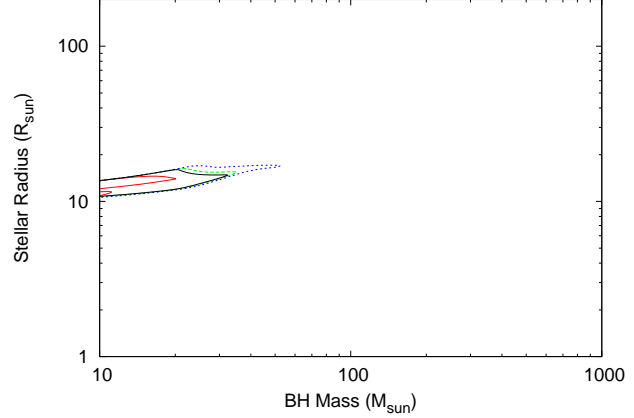
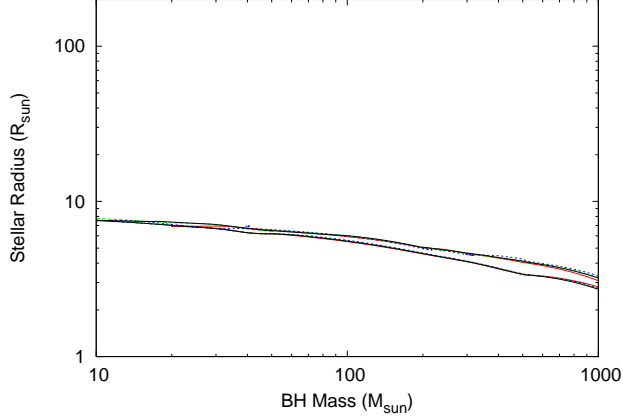
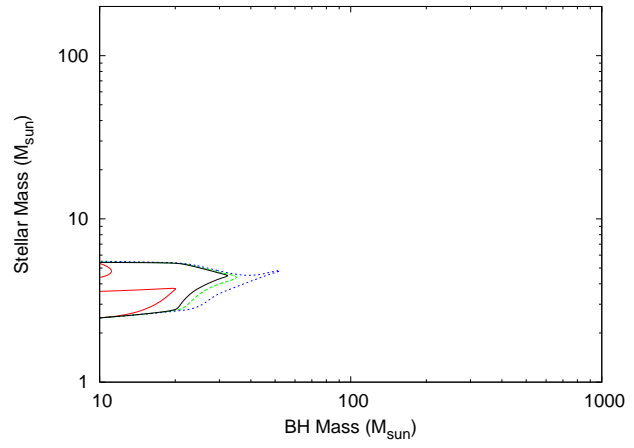
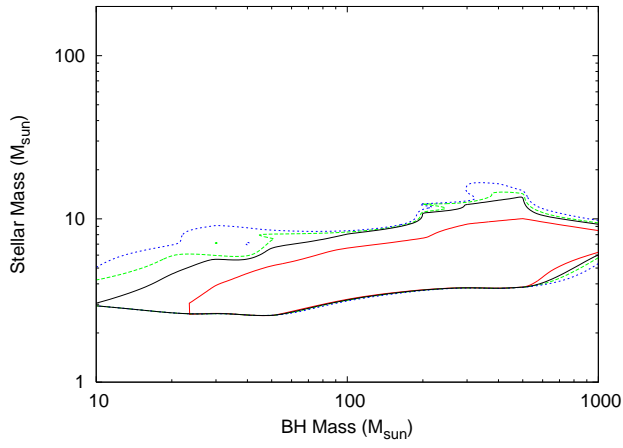
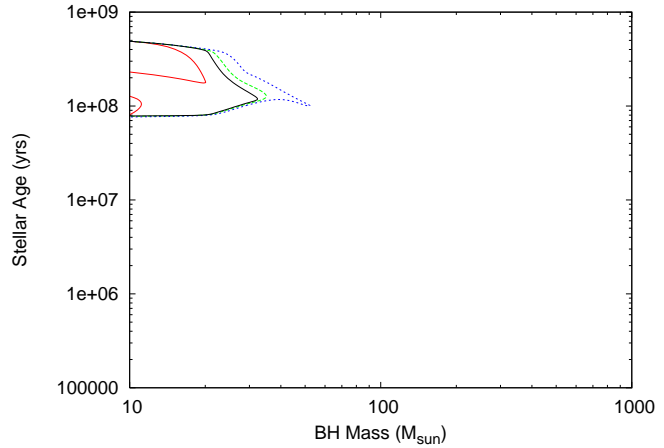
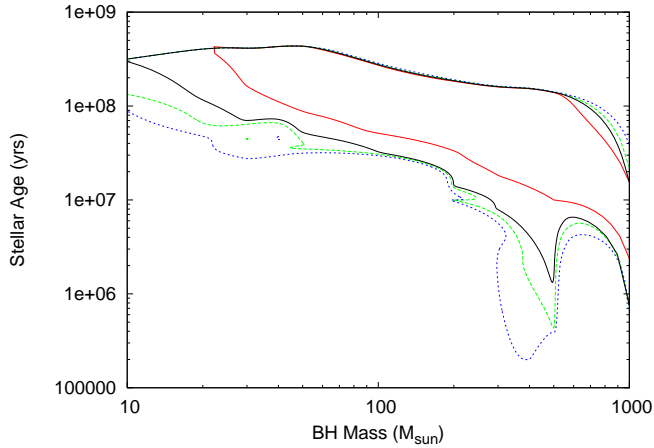


Figure 3. Confidence contours for the binary parameters for the source X-6 in M81. We assume a binary inclination of $\cos(i) = 0.5$, superior conjunction with respect to the observer and the star, and a stellar metallicity of $Z = 0.2Z_{\odot}$. We use an X-ray hardness ratio of $\xi = 0.01$. The red, black, green and blue lines denote the 68%, 90%, 95% and 99% confidence intervals respectively.

A very massive ($> 80M_{\odot}$) donor is also possible when we use a low BH mass.

3.6 ULX X-2 in NGC 1313

Mucciarelli et al. (2005) analysed archive ESO VLT photo-

Figure 4. As for Figure 3, but with a binary inclination of $\cos(i) = 0.0$ and a hardness ratio of $\xi = 0.1$.

metric data of this $L_x = 10^{40} \text{ erg s}^{-1}$ ULX. They found two possible candidates for the optical counterpart of this ULX within the *Chandra* error circle. They gave B, V and R magnitudes for the candidate designated C1 in that paper, and V and R magnitudes for the candidate C2. This second candidate was not detected in the B-band.

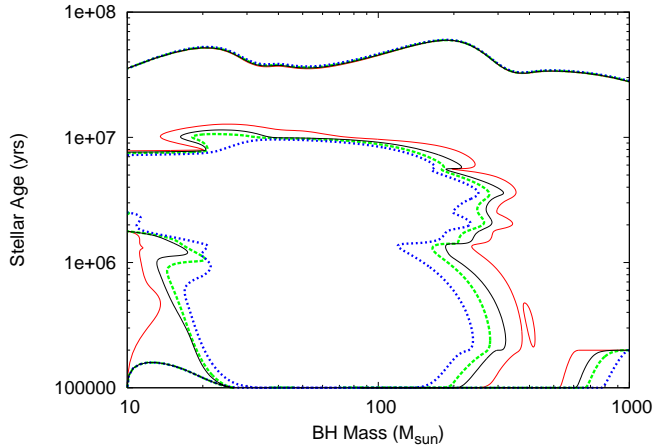


Figure 5. Confidence contours for the binary parameters for the ULX in NGC 5408. We assume a binary inclination of $\cos(i) = 0.5$, superior conjunction with respect to the observer and the star, and a stellar metallicity of $Z = 0.2Z_{\odot}$. We use an X-ray hardness ratio of $\xi = 0.1$. The red, black, green and blue lines denote the 68%, 80%, 95% and 99% confidence intervals respectively.

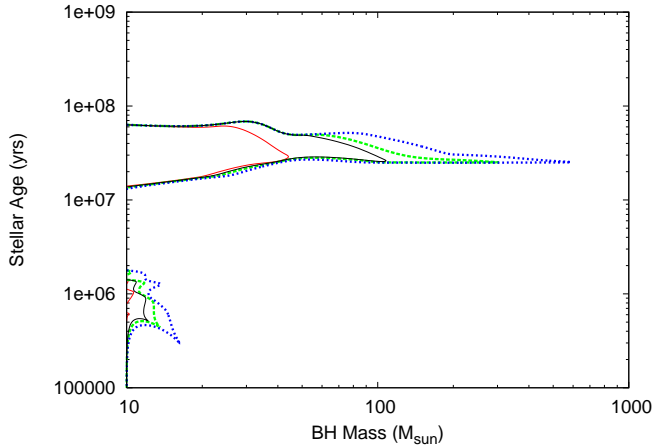


Figure 6. As for Figure 5, but with a binary inclination of $\cos(i) = 0.0$.

We applied our model to the photometric data of both candidates. We find the non-detection of C2 in the B-band makes it inconsistent with being an irradiated donor star and/or disc. We therefore take candidate C1 to be the counterpart. This determination has been confirmed by a recent, more accurate astrometric study with the *HST* ACS instru-

ment (Liu et al. 2007). We see in Figure 7 that an upper bound of $100M_{\odot}$ exists for this source when we set the inclination to be $\cos(i) = 0.5$. If we take Figures 7 and 8 together we see that the donor star mass ranges from 6 to $38M_{\odot}$, with the upper bound decreasing to $23M_{\odot}$ in the $\cos(i) = 0.5$ case. For $\cos(i) = 0.5$ the radius is $3 - 6R_{\odot}$.

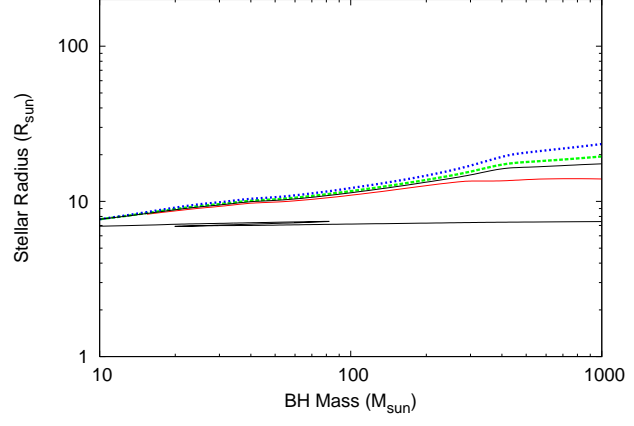
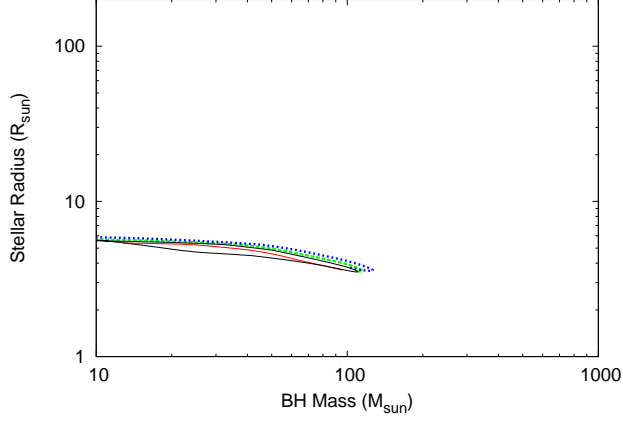
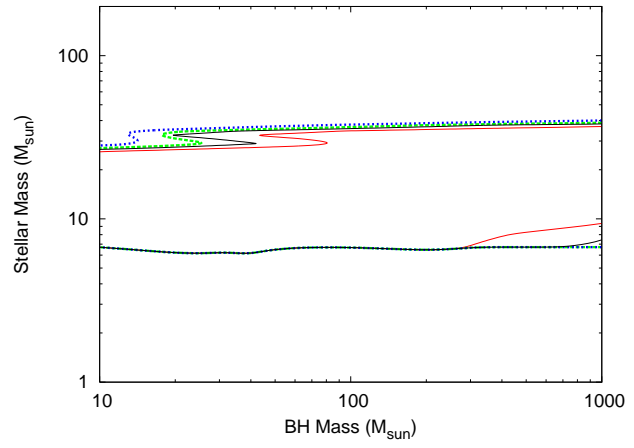
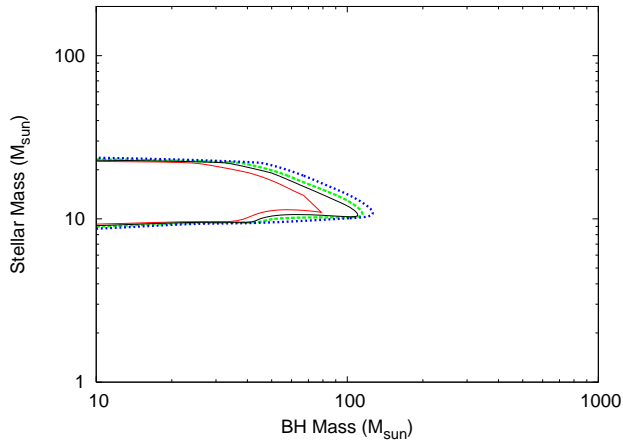
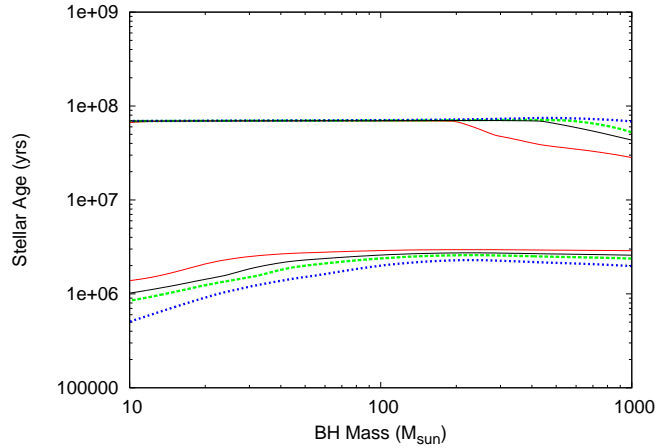
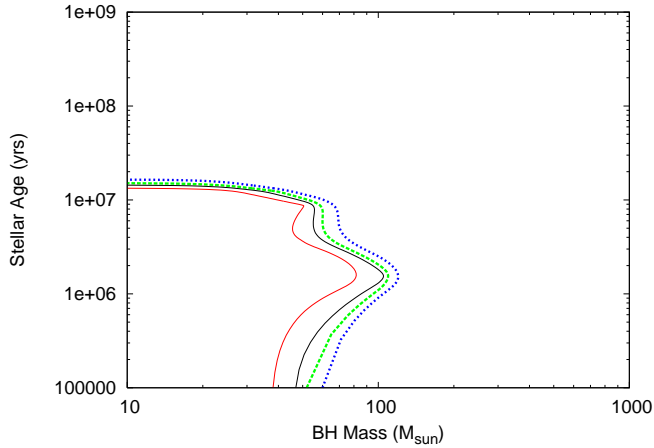


Figure 7. Confidence contours for the binary parameters for ULX X-2 in NGC 1313, assuming candidate C1 is the optical counterpart. We assume a binary inclination of $\cos(i) = 0.5$, superior conjunction with respect to the observer and the star, and a stellar metallicity of $Z = 0.2Z_\odot$. We use an X-ray hardness ratio of $\xi = 0.1$. The red, black, green and blue lines denote the 68%, 90%, 95% and 99% confidence intervals respectively.

Setting $\cos(i) = 0.0$ results in the radius increasing to $7 - 18R_\odot$.

Figure 8. As for Figure 7, but with a binary inclination of $\cos(i) = 0.0$.

3.7 ULX in Holmberg II

This ULX has an X-ray luminosity measured at up to 10^{40}erg s^{-1} (Kaaret et al. 2004), although it is highly variable. It is associated with a diffuse, photoionised nebula,

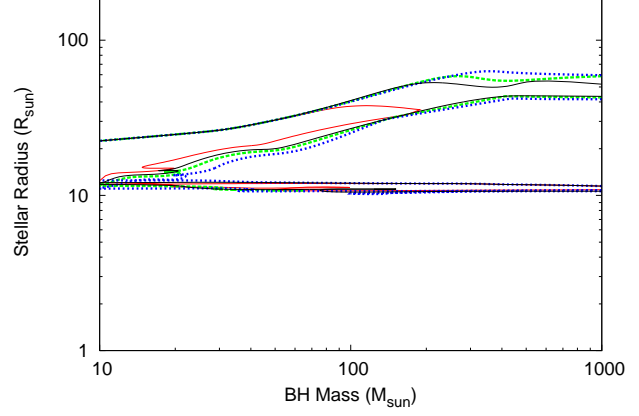
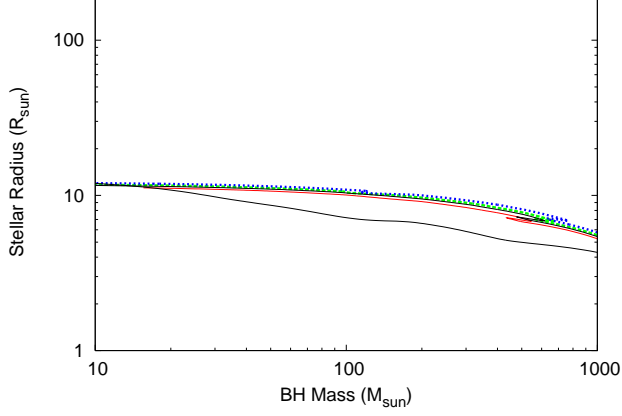
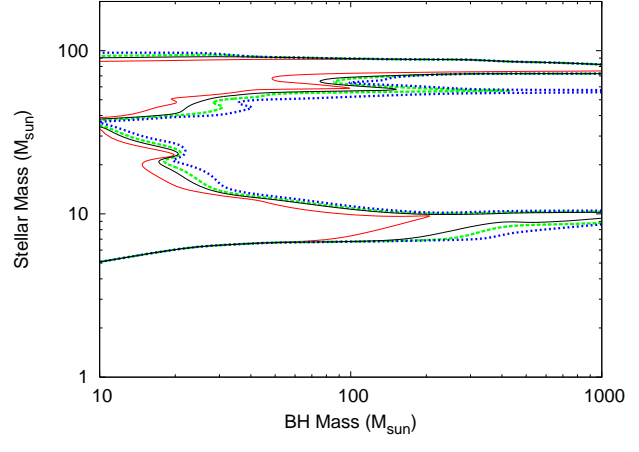
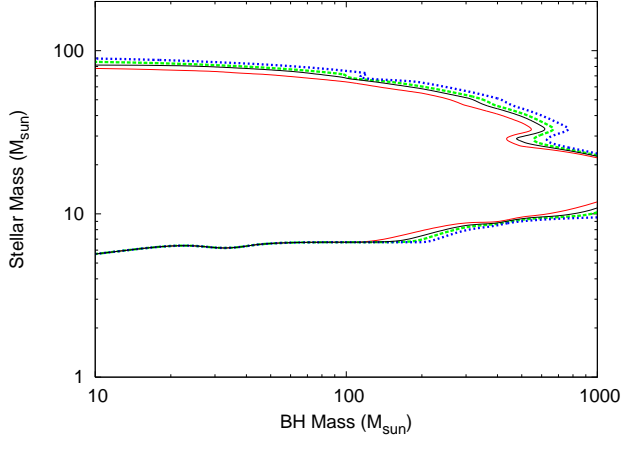
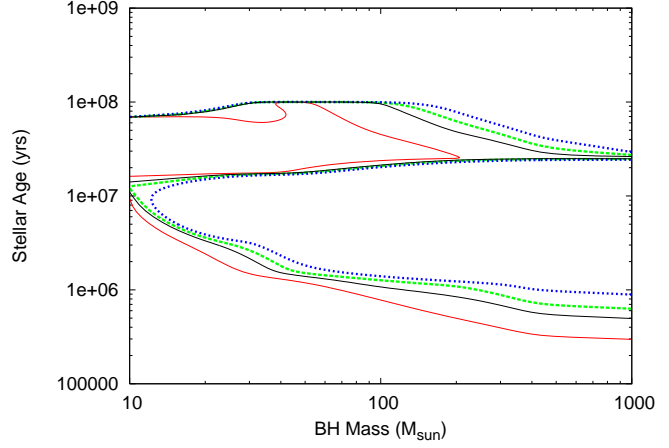
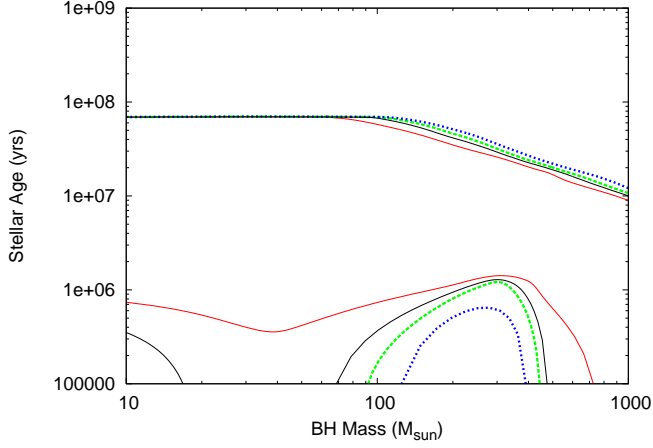


Figure 9. Confidence contours for the binary parameters for the ULX in Holmberg II. We assume a binary inclination of $\cos(i) = 0.5$, superior conjunction with respect to the observer and the star, and a stellar metallicity of $Z = 0.2Z_{\odot}$. We use an X-ray hardness ratio of $\xi = 0.1$. The red, black, green and blue lines denote the 68%, 90%, 95% and 99% confidence intervals respectively.

whose energetics suggests that the X-ray emission from the accreting source is truly luminous and not strongly beamed. Kaaret et al. (2004) gives both the V magnitude of the counterpart and its (B-V) colour.

We find the available optical data does not allow us to constrain the BH mass for any orientation. As regards the

Figure 10. As for Figure 9, but with a binary inclination of $\cos(i) = 0.0$.

parameters of the donor star, we see in Figure 9 that if we set $\cos(i) = 0.5$ the stellar age and mass are quite poorly constrained, with the mass ranging from 6 to $82M_{\odot}$ and the age ranging from 10^5 to $10^{7.85}$ yr. The stellar radius is better defined, and lies between 4 and $12R_{\odot}$.

For the $\cos(i) = 0.0$ case (Figure 10), the picture is

more complicated. Our results suggest two possibilities for the donor star parameters. It can either be a star of mass $37 - 92M_{\odot}$ and radius $10 - 12R_{\odot}$, or a much older object with mass $5 - 34M_{\odot}$ and radius $12 - 55R_{\odot}$. These two possibilities are more tightly constrained as the BH mass increases.

4 DISCUSSION

4.1 Classification of the donor stars

In Table 2 we list the Zero Age Main Sequence (ZAMS) stellar masses and temperatures we calculate for the donor stars in the seven systems we have investigated. These values do not account for any loss due to the mass accretion, and so should be increased by an amount depending on when the mass transfer began. In Table 3 we list the most likely currently observed spectral type we obtained for each source. We find the donor stars are in general consistent with main sequence or evolved giant/supergiant stars of type B, except in the NGC 5204 ULX. Not surprisingly, we find the donor stars to be larger, less massive and older than inferred when irradiation is not taken into account. We can also rule out donors of type A or later in most cases. We now comment on individual sources, giving the currently observed spectral type in each case.

For ULX X-7 in NGC 4559, our determination of the mass and radius suggest the star is a supergiant, of spectral type B (if we assume an inclination such that there is a disk component to the emission) or spectral type A (if we assume the plane of the disk is perpendicular to the sky – $\cos(i) = 0.0$). The donor has an age and mass consistent with the stars in its immediate neighbourhood (Soria et al. 2005).

Liu et al. (2002) found the photometric observations of the counterpart to M81 X-6 fitted with an MS O-star. They noted that although the photometric data can be fit by considering an O9 MS star the colour of the data is redder than would be expected. They corrected for this by assuming intrinsic extinction by the dusty environment of the ULX, which changed their determination of the spectral type to an O8 star. We argue instead that the red excess could be explained in terms of a disc component adding to the optical emission (as in LMC X-3, van Paradijs et al. 1987). The stellar parameters we calculate instead identify the donor as an MS or giant evolved B-star.

For the ULX in NGC 5408, our best fit model is a giant, evolved B star, but we cannot rule out the possibility of very massive ($> 45M_{\odot}$) O-type donor star. When we assume the inclination is such that the plane of the disk is perpendicular to the plane of the sky, the radius implied by our model increases, and matches that of a B-type supergiant.

For ULX X-2 in NGC 1313, our calculations suggest the candidate designated C1 in Mucciarelli et al. (2005) is most likely to be the optical counterpart. The low stellar radius we find from the model fit suggest the donor is a main sequence star. The most likely spectral type is B, although a late O-type is also a possibility, especially when we set $\cos(i) = 0.0$. Mucciarelli et al. (2005) suggest that the donor is an MS star of type O9 – B0, which is consistent with our findings.

For the Holmberg II ULX, when we set $\cos(i) = 0.5$ we find a tight constraint on the stellar radius but a large mass

range. These results are consistent with the donor being either an MS O-star or a giant B-star. We see two distinct possibilities in the $\cos(i) = 0.0$ case as well, but here the solutions corresponding to a lower stellar mass give a higher stellar radius, so the donor can be classified as either an MS O-star or a B supergiant. Kaaret et al. (2004) suggested the donor was of type O4V or B3Ib, which is consistent with our findings.

For the ULX in NGC 5204, Liu et al. (2004) reported the multi-band photometry to be consistent with stars of type O5 V, O7 III or B0 Ib. They also reported *HST/STIS* far-ultraviolet spectral observations, and on the basis of those they suggest the star is most likely to be of type B0 Ib, although they note the spectrum does contain some peculiarities for a star of this type. The STIS data are also consistent with the presence of an X-ray illuminated accretion disc. Our model does not provide good fits, because we have applied a constraint in which the mass accretion rate is fixed. When we relax this constraint we find the observation is consistent with a very massive O-type MS star, and a mass accretion rate of an order of magnitude or more greater than we expect from the observed X-ray luminosity.

The conclusion that the donor is an MS O-star disagrees with Liu et al. (2004), (and this would be the only source where we have found the donor to be a more massive and compact star than originally thought). Liu et al. (2004) found the photometric observations to be consistent with an MS or giant O-type donor star, but concluded that the star is a B-type supergiant is based on the additional *HST STIS MAMA/FUV* data. Specifically, the equivalent width of the $\text{Si}_{III} \lambda 1299$ line is suggestive of a star cooler than 25000K. An MS O-star would be hotter than this, even on its unirradiated hemisphere. If we assume our interpretation of the optical data is correct, we must therefore suggest that this line originates somewhere other than on the surface of the star, or that the surface layers are modified by the Roche lobe and material loss by accretion.

For the ULX in M101, we find the donor to be a B-type star if the optical emission has an observable disk and a star component. If the disk is perpendicular to the plane of the sky, we have the same mass accretion constraint problem as for the NGC 5204 ULX. If we relax this constraint, the observation is consistent with the donor being a late O or B supergiant, or possibly an MS O star.

4.2 Comments on mass accretion rate constraints

In the NGC 5204 ULX we have found that the mass accretion rate as inferred from the nuclear evolution timescale (via the evolutionary tracks) is larger than we would infer from the X-ray luminosity. We can explain this in one of three ways. Firstly, we can assume that our interpretation of the optical data is correct and the donor is an MS O-star. This implies that the accretion efficiency $\eta \sim 0.01$, an order of magnitude less than for standard disk accretion. Mass outflows or advective inflows are well-known possible reasons for sub-standard accretion efficiency.

The second possibility is that the BH is mostly fed by stellar winds rather than Roche lobe overflow. This would invalidate both the geometry used in our model and our calculation of the mass accretion rate, since both of them are dependent on Roche lobe overflow as the accretion mech-

anism. Given that this source is a lower-luminosity ULX ($3 \times 10^{39} \text{ erg s}^{-1}$) when compared to the others in our sample, a supergiant donor feeding the ULX via a wind is a reasonable possibility. However, this is inconsistent with the findings of Liu et al. (2004), as they report the FUV spectrum shows evidence of Roche lobe overflow.

A third possibility is that these objects are confused at some level in current observations at optical wavelengths, with more than one star contributing to an unresolved counterpart.

For the ULX in M101, we have the same problem as for the NGC 5204 ULX if the inclination of the system is set to $\cos(i) = 0.0$. We can explain this by ruling out an inclination of $\cos(i) = 0.0$ in this case. Alternatively, this can be explained by either of the three possibilities detailed above. Given that this source has the weakest X-ray luminosity ($1 \times 10^{39} \text{ erg s}^{-1}$) of those in our sample, the possibility that this system is wind fed is relatively more likely.

4.3 Constraining the BH mass

A key to understanding the nature of ULXs is the determination of the BH mass. In five out of seven systems, we can constrain the mass of the BH based on the optical observations, for certain inclinations. We list these five cases in Table 4.

If we assume the ULX X-7 in NGC 4559 has an inclination of $\cos(i) = 0.0$, we find an upper limit on the BH mass of $\simeq 35M_{\odot}$. Analysis of the X-ray data has suggested a lower limit on the BH mass of $50M_{\odot}$ (Cropper et al. 2004). This inconsistency can be accounted for by inclining the binary system in our model so that the optical emission includes a disk component. This results in the upper limit on the BH mass increasing. We see in Figure 1 that for an inclination of $\cos(i) = 0.5$ the upper limit has disappeared.

When we assume an inclination of $\cos(i) = 0.5$ for the ULX in NGC 1313, we find an upper limit on the BH mass of $100M_{\odot}$. This upper limit increases as the disk component is reduced, and vanishes when we set $\cos(i) = 0.0$. This BH range is consistent with a BH mass of $\sim 100M_{\odot}$ previously inferred from the X-ray data (Zampieri et al. 2004).

If we use an inclination of $\cos(i) = 0.0$ for the ULX in NGC 5408, we find a maximum BH mass of $110M_{\odot}$. When we incline the system so as to include a disk component, the upper limit disappears. In both cases this is consistent with the X-ray data, which implies a BH mass of $\sim 100M_{\odot}$, assuming accretion at the Eddington limit (Soria et al. 2004).

We note also that the ULX in NGC 5204 has a maximum BH mass of $\simeq 240M_{\odot}$ when we assume an inclination of $\cos(i) = 0.5$ and a very low accretion efficiency. The constraint disappears when we set $\cos(i) = 0.0$. The X-ray data supports the presence of a cool thermal disk component (Roberts et al. 2005) which may be produced by an IMBH or by a stellar-mass disk cooled by other processes. Unfortunately, optical mass constraints are not strong enough to discriminate between the stellar-mass and IMBH scenarios.

The fifth source for which we have a BH mass constraint is ULX X-6 in M81. We see that when we set $\cos(i) = 0.0$ there is an upper limit on the BH mass of $33M_{\odot}$, but if we set $\cos(i) = 0.5$ we find a lower limit on the BH mass of $20M_{\odot}$. The existence of this lower limit is dependent on the irradiating X-ray spectrum being softer than we have else-

where assumed and the age of the donor being comparable to the of the field stars. We note also that this BH has been suggested to have a mass of $18M_{\odot}$ based on analysis of X-ray data (Liu et al. 2002), but the authors found it to be model dependent.

4.4 Predictions for further opt/IR observations

We now look at what these new identifications for the donor stars mean for future optical observations of these sources. We show our predictions for the binary periods of the seven systems in Table 5. The ULX in M81 is a good prospect for determination of the BH mass, so we base this discussion around this source. Liu et al. (2002) suggested the donor star was of type O8V/O9V. A typical O8V star has a mass of $23M_{\odot}$ and a radius of $8.5R_{\odot}$. Assuming a Roche-lobe filling donor, the binary period for such a source will be $\simeq 39$ hours if we assume a $10M_{\odot}$ BH and $\simeq 44$ hours if we assume a $1000M_{\odot}$ BH. The amplitude of the optical lightcurve will be dependent on the BH mass, binary inclination and other parameters, but in figure 3 of Copperwheat et al. (2005) we see that the optical amplitude of the lightcurve of a typical O-star irradiated by an X-ray source of $L_x = 10^{40} \text{ erg s}^{-1}$ is of the order of a tenth of a magnitude.

As we see in Table 5, our predictions for the binary period of the M81 ULX change significantly with both inclination and BH mass. A measured period of $\sim 100 - 300$ hours would imply an inclination of close to $\cos(i) = 0.0$ and a low ($\sim 10M_{\odot}$) BH mass. A shorter period would imply both a more face-on system and a more massive BH, with a period of around 16 hours suggesting a BH mass of $1000M_{\odot}$. We note also that the donor star in the $\cos(i) = 0.0 / 10M_{\odot}$ case is a larger, more evolved object. We would expect the variation in optical luminosity to be observable in this case, since the variation is not diluted by the accretion disk, and the optical luminosity of evolved stars is more significantly modified by X-ray irradiation than for MS stars (Copperwheat et al. 2005). A small or unobservable optical variation would imply an inclined system, an MS donor and a more massive BH.

In Copperwheat et al. (2005) we noted that infrared observations might be an important diagnostic in determining the nature of ULXs. We illustrate this point in Figure 11. We show here colour-magnitude diagrams for B against $(B - V)$ and H against $(H - K)$ for the optical counterpart to the ULX in NGC 5408. In both cases, we plot the sections of the evolutionary tracks which fit the optical data to the 90% confidence level. We plot tracks for inclinations of $\cos(i) = 0.5$ and $\cos(i) = 0.0$ with the star in superior conjunction. In the B versus $(B - V)$ plot, the sets of tracks for the two inclinations are necessarily similar in colour and magnitude. However, we see that at infrared wavelengths there is a clear distinction between the $\cos(i) = 0.5$ tracks and the $\cos(i) = 0.0$ tracks in both colour and magnitude. It is clear therefore that the combination of IR and optical observations will allow us to constrain parameters in ULX systems with much higher precision.

4.5 The evolution and history of ULXs

If IMBHs do indeed exist, it is of great importance to clarify how the ULX/IMBH and the star formation process in their

Table 2. Calculated stellar ZAMS parameters for the donor stars. These values do not account for any loss due to the mass accretion, and so should be increased by an amount depending on when the mass transfer began (* applies only when we do not apply a constraint on the mass accretion rate. ** applies only for a hardness ratio of $\xi = 0.01$.)

	BH Mass = $10M_{\odot}$		BH Mass = $100M_{\odot}$		BH Mass = $1000M_{\odot}$	
	Mass (M_{\odot})	Log Temp (K)	Mass (M_{\odot})	Log Temp (K)	Mass (M_{\odot})	Log Temp (K)
NGC 4559 X-7						
$\cos(i) = 0.5$, superior conjunction	5.08 – 12.19	4.30 – 4.48	5.08 – 9.80	4.30 – 4.44	5.67 – 20.73	4.32 – 4.57
$\cos(i) = 0.5$, inferior conjunction	5.68 – 12.68	4.32 – 4.49	5.68 – 9.11	4.32 – 4.42	5.67 – 20.73	4.32 – 4.57
$\cos(i) = 0.0$, superior conjunction	5.97 – 12.77	4.33 – 4.49	–	–	–	–
M81 X-6						
$\cos(i) = 0.5$, superior conjunction **	–	–	3.38 – 7.10	4.20 – 4.37	6.36 – 9.10	4.35 – 4.42
$\cos(i) = 0.5$, inferior conjunction **	–	–	2.56 – 8.03	4.12 – 4.39	6.56 – 9.10	4.35 – 4.42
$\cos(i) = 0.0$, superior conjunction	2.48 – 5.37	4.11 – 4.31	–	–	–	–
NGC 5204 ULX						
$\cos(i) = 0.5$, superior conjunction *	68.4 – 109.3	4.71 – 4.74	72.0 – 95.3	4.71 – 4.73	–	–
$\cos(i) = 0.5$, inferior conjunction *	69.4 – 110.3	4.71 – 4.74	72.0 – 95.3	4.71 – 4.73	–	–
$\cos(i) = 0.0$, superior conjunction *	65.1 – 116.3	4.70 – 4.75	69.6 – 117.3	4.71 – 4.75	73.4 – 118.3	4.71 – 4.75
M101 ULX-1						
$\cos(i) = 0.5$, superior conjunction	2.46 – 4.13	4.11 – 4.24	2.48 – 4.81	4.11 – 4.28	2.93 – 6.35	4.16 – 4.35
	81.3 – 84.3	4.72				
$\cos(i) = 0.5$, inferior conjunction	3.24 – 4.03	4.18 – 4.24	2.94 – 4.58	4.16 – 4.27	2.93 – 6.35	4.16 – 4.35
	81.3 – 84.3	4.72			45.0 – 52.4	4.67 – 4.69
$\cos(i) = 0.0$, superior conjunction *	15.7 – 101.3	4.52 – 4.74	19.0 – 100.4	4.56 – 4.74	15.7 – 104.3	4.52 – 4.74
NGC 5408 ULX						
$\cos(i) = 0.5$, superior conjunction	5.08 – 23.49	4.30 – 4.59	5.68 – 18.98	4.32 – 4.56	8.32 – 57.4	4.40 – 4.69
	68.4 – 117.3	4.71 – 4.75	84.3 – 88.3	4.72 – 4.73		
$\cos(i) = 0.5$, inferior conjunction	5.37 – 14.3	4.31 – 4.51	5.67 – 19.0	4.32 – 4.56	8.32 – 57.4	4.40 – 4.69
	70.4 – 117.3	4.71 – 4.75	86.3 – 88.3	4.72 – 4.73		
$\cos(i) = 0.0$, superior conjunction	5.08 – 14.35	4.30 – 4.51	9.80	4.44	–	–
	79.2 – 117.3	4.72 – 4.75				
NGC 1313 X-2						
$\cos(i) = 0.5$, superior conjunction	9.29 – 23.1	4.42 – 4.59	10.3 – 12.1	4.45 – 4.48	–	–
$\cos(i) = 0.5$, inferior conjunction	6.71 – 27.11	4.36 – 4.61	11.0 – 15.3	4.46 – 4.52	–	–
$\cos(i) = 0.0$, superior conjunction	5.68 – 26.11	4.32 – 4.61	5.37 – 35.5	4.32 – 4.65	7.56 – 37.5	4.38 – 4.65
Holmberg II ULX						
$\cos(i) = 0.5$, superior conjunction	5.68 – 81.4	4.32 – 4.72	6.71 – 68.4	4.36 – 4.71	10.82 – 22.1	4.45 – 4.58
$\cos(i) = 0.5$, inferior conjunction	5.68 – 88.3	4.32 – 4.73	5.67 – 68.4	4.32 – 4.71	10.82 – 22.1	4.45 – 4.58
$\cos(i) = 0.0$, superior conjunction	5.08 – 90.3	4.30 – 4.73	4.81 – 9.11	4.28 – 4.42	10.28	4.45
			57.2 – 88.3	4.70 – 4.73	72.3 – 84.3	4.71 – 4.72

Table 3. Spectral type of the donor stars. We compare the classification given by previous authors (as listed in table 1) with our determination of the current and ZAMS spectral types. We give the most likely type in each case - we elaborate on this in the text. (* applies only when we do not apply a constraint on the mass accretion rate.). References: ¹Soria et al. (2005), ²Liu et al. (2002), ³Liu et al. (2004), ⁴Kuntz et al. (2005), ⁵Mucciarelli et al. (2005), ⁶Kaaret et al. (2004).

	Previous spectral type	Our determination		
		Current	ZAMS	
NGC 4559 X-7	O / B supergiant ¹	Late B – A giant/supergiant	B5 – B0	
M81 X-6	O8V / O9V ²	B MS/giant	B9 – B2	
NGC 5204 ULX	B0Ib ³	O MS *	O5 or earlier *	
M101 ULX-1	B supergiant ⁴	A/B MS/giant	A0 – O4	
NGC 5408 ULX	–	B giant/supergiant (or O MS)	B4 or earlier	
NGC 1313 X-2	B0 – O9 MS ⁵	B MS	B6 – O6	
Holmberg II ULX	O4V / B3Ib ⁶	B giant/supergiant (or O MS)	B5 or earlier	

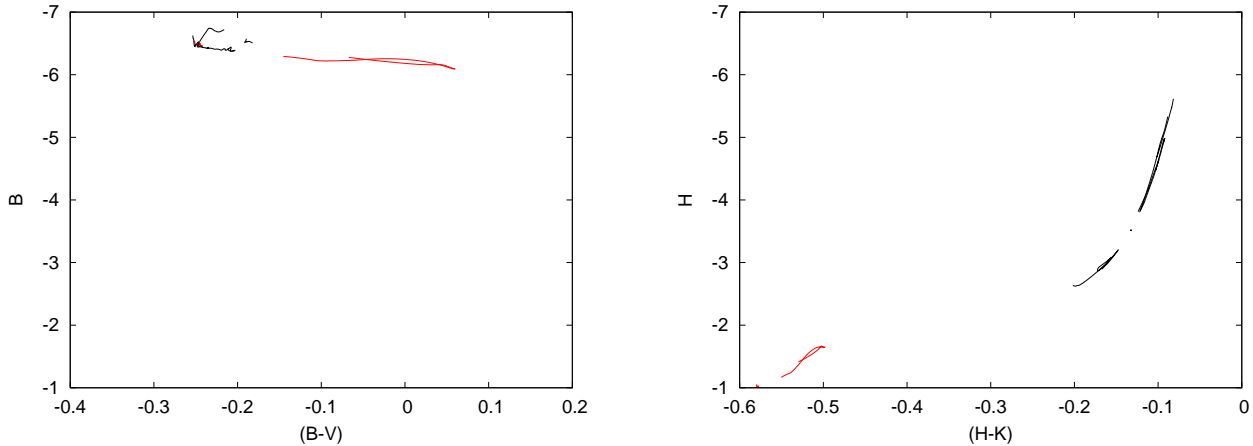


Figure 11. Colour-magnitude diagrams showing the 90% confidence contours for the optical counterpart of the ULX in NGC 5408, for inclinations of $\cos(i) = 0.5$ (black) and $\cos(i) = 0.0$ (red) with the star in superior conjunction.

Table 4. BH mass constraints, and the inclination for which they apply (* applies only when we do not apply a constraint on the mass accretion rate. ** applies only for a hardness ratio of $\xi = 0.01$.)

NGC 4559 X-7	$< 35M_{\odot}$ for $\cos(i) = 0.0$
M81 X-6	$> 20M_{\odot}$ for $\cos(i) = 0.5$ **
	$< 33M_{\odot}$ for $\cos(i) = 0.0$
NGC 5204 ULX	$< 240M_{\odot}$ for $\cos(i) = 0.5$ *
NGC 5408 ULX	$< 110M_{\odot}$ for $\cos(i) = 0.0$
NGC 1313 X-1	$< 100M_{\odot}$ for $\cos(i) = 0.5$

Table 5. Predictions of the orbital periods in these systems, in hours, based on our determinations of the donor star parameters (* applies only when we do not apply a constraint on the mass accretion rate. ** applies only for a hardness ratio of $\xi = 0.01$.)

BH mass	$10M_{\odot}$	$100M_{\odot}$	$1000M_{\odot}$
$\cos(i) = 0.5$, superior conjunction			
NGC 4559 X-7	418 – 732	260 – 276	67.0 – 78.8
M81 X-6 **	–	47.9 – 59.5	15.9 – 16.2
NGC 5204 ULX *	27.4 – 42.0	37.8 – 44.5	–
M101 ULX-1	767 – 873	271 – 295	77.6 – 82.9
	26.6 – 26.9		
NGC 5408 ULX	114 – 277	94.9 – 112	33.4 – 36.6
	27.5 – 39.3	37.1 – 37.4	
Holmberg II ULX	27.2 – 152	35.4 – 61.5	21.1 – 22.1
NGC 1313 X-2 C1	22.6 – 36.4	21.8 – 27.4	–
$\cos(i) = 0.0$, superior conjunction			
NGC 4559 X-7	864 – 2060	–	–
M81 X-6	136 – 287	–	–
NGC 5204 ULX *	27.5 – 46.7	38.8 – 56.4	41.8 – 57.7
M101 ULX-1 *	27.2 – 387	38.2 – 394	40.6 – 376
NGC 5408 ULX	247 – 732	760	–
	27.5 – 41.0		
Holmberg II ULX	27.0 – 417	542 – 1500	783
		35.3 – 37.3	36.2 – 38.5
NGC 1313 X-2 C1	26.0 – 96.2	28.4 – 157.5	28.3 – 190.4

vicinity are related. The open question to resolve is whether the donor star is coeval to the BH progenitor or captured by the BH some time after formation. If the star and the BH formed together, determining the age of the donor star also determines the age of the BH. If the star was captured by the BH, then the statistics of the spectral type and mass distribution of the donor stars can be used to set constraints on the capture rate and hence provide estimates to the IMBH populations.

In our study, we found that the donor stars are mainly of spectral type B, and are significantly older than previously determined. For example, Liu et al. (2002) inferred the donor star in M81 X-6 ULX to have an age of less than $10^{6.7}$ yr. We find the minimum stellar age to be an order of magnitude greater, if the BH mass is assumed to be $< \sim 100M_{\odot}$. In a number of cases, the photometric data alone allows us to infer the donor is of spectral type B. In other cases, a range of (more massive) possibilities exist, but by applying constraints on the mass accretion rate we find a B-type star to be the most likely donor. In the case where the optical data points to a massive, O-type donor, the implied mass accretion rate is inconsistent with that which would be expected from the X-ray observation, given our assumed accretion efficiency of $\eta = 0.1$. We suggest therefore, that donor stars of a narrow spectral and mass range are necessary to produce a very luminous, Roche lobe fed ULX, and our finding of large fraction of B-type stars in the ULX sample may be significant.

If the compact objects in these systems are indeed IMBHs, and if we assume the capture scenario, then the fact that a B-type donor is sufficient to fuel a ULX allows a lower spatial density for IMBHs for the observed population of ULXs than if the donors were found to be of type O, since B-type stars are more common and so the chances of forming a ULX binary are higher. Various authors have modelled the tidal capture of a donor star by an IMBH (see e.g Hopman, Portegies Zwart & Alexander 2004; Blecha et al. 2006). The capture rate appears to be \sim stellar number density, but is only weakly dependent on stellar mass. This would imply that more B stars than O stars should be captured. However, a competing effect is the re-

quirement that the star comes close enough to be captured but far enough not to be tidally destroyed. This requirement may favour O stars, since they may more easily survive tidal squeezing. We note also that tidal capture of isolated stars is only one process through which an IMBH might acquire a companion; another process is by capturing stars in binary systems, which may have a different frequency of occurrence and period distribution for B or O stars.

It is also interesting to note that the two lowest luminosity ULXs in our sample, those in M81 and M101, are also those where an old, less massive donor of age $\sim 10^8$ Myr is a possibility. This may be related to the existence of a population of low-luminosity sources ($<\sim 2 \times 10^{39}$ erg s $^{-1}$) also found in old elliptical galaxies, probably identified as low-mass XRBs. Conversely, the ULXs more luminous than 2×10^{39} erg s $^{-1}$ are almost always found in star-forming galaxies, and we find the donor stars to be of age $\sim 10^7$ Myr or less.

4.6 Other systematic effects

We have made a number of assumptions in this work. We reexamine here some of the effects that will have an influence on our conclusions.

4.6.1 System geometry

We have assumed a thin disk in our model, but as we noted in Section 1, some authors have suggested more complicated disk models, with a thin disk covered by a Comptonised corona (Socrates & Davis 2005). These models have been developed to support the possibility of super-Eddington accretion in ULX systems. The corona emits hard X-rays which are reflected by the ionized surface of the inner disk. As in our disk model, the bulk of the optical emission comes from the outer regions of the disk, due to these regions having a much larger surface area than the inner parts of the disk. To a large extent therefore the optical/IR emission is similar. However, the corona model will result in a harder X-ray spectrum incident on the outer disk. We discuss the effect of changing the X-ray hardness in more detail in Section 4.6.3. Additionally, since the corona extends away from the disk surface the angles of incidence of the X-rays on the outer disk regions are changed somewhat, but the extent of the corona is not large enough for this to have a significant effect.

4.6.2 Radiation pressure

In the results we have presented here, we have not included the effects of radiation pressure. The effects of radiation pressure on the shape of a Roche lobe filling star are unclear: some authors suggest that the shape will be unaffected (Howarth 1997), whereas others predict a significant effect in very X-ray luminous binaries (Phillips & Podsiadlowski 2002). We showed in Copperwheat et al. (2005) that under the Phillips & Podsiadlowski (2002) formulation, radiation pressure has an increasing effect on the shape and luminosity of the donor as the BH mass is decreased. This is because as we decrease the BH mass the binary separation also decreases, and the X-ray flux incident on the stellar surface

increases. We found also that the effect decreases as we use a donor of later spectral type, for the same reasons. We find therefore that for most of our fitted solutions, where the BH mass lies between 100 and $1000M_\odot$ and the donor is found to be a star of type B or later, the effect of including radiation pressure on our results is small. We begin to see an appreciable deviation from the results we have reported when we use a BH mass of $\sim 100M_\odot$ and a main sequence, O-type donor. Even in this case, the fitted stellar mass only changes by 1 or $2M_\odot$, which is a small percentage of the total stellar mass and not enough to alter our classification of the star. We would expect a more significant deviation for low ($\sim 10M_\odot$) BH masses, but the Phillips & Podsiadlowski (2002) formulation we use for radiation pressure becomes inappropriate at this point, since it does not allow for any circulatory currents in the stellar surface driven by the irradiation. This means it tends to represent an extreme case of maximum stellar distortion, and in this extreme case the radiation pressure is very large, to the point of stripping the outer layers away from the donor so that it looks quite unlike an ordinary star. A radiation pressure formulation which included circulatory currents would predict a lessened effect on the stellar shape. Shielding by the disk will mitigate this effect further.

Given that the actual effect of radiation pressure on the stellar shape in ULX systems is not fully understood, we consider our omission of this component in this paper to be appropriate. We do however note this introduces an additional source of uncertainty, particularly for low BH masses.

4.6.3 X-ray hardness

The hardness of the X-ray spectrum determines the depth at which the incident radiation deposits most of the energy. Soft X-rays are easily absorbed at the disk surface, while hard X-rays attenuate only at large optical depths. For incident X-rays with a soft spectrum, a hot surface skin layer is formed at depths optically thin to optical radiation, and the emission from the skin layer is at wavelengths shortward of the optical bands. However, for incident X-rays with a hard spectrum, most of the energy is deposited at depths optically thick to optical radiation. This heats the internal regions of the disk plane and hence leads to a more luminous disk at the optical wavelengths. This was illustrated in figure 6 of Copperwheat et al. (2005), where we see that as the X-ray hardness is increased, the disk V magnitude similarly increases. We noted also that the effect of varying the hardness ratio on the stellar luminosity was very small.

Because we do not know the hardness of the X-ray spectrum incident on the irradiated surfaces in these systems (as discussed in Section 2.1) we have used a fixed hardness ratio of $\xi = 0.1$. We now discuss the effect of varying the hardness ratio on our results.

In Figure 12 we have plotted our determinations of the masses and radii of the donor stars in the NGC 4559 and NGC 5408 ULXs. We have fixed the inclination to $\cos(i) = 0.5$, the BH mass to $100M_\odot$ and the stellar age to 10 Myr. If we examine the results for the ULX in NGC 4559, we see that varying ξ has little to no effect on our determination of the mass of the donor star. Our determination of the radius however, decreases with increasing hardness ratio. We see a similar decrease in stellar radius with increasing ξ in

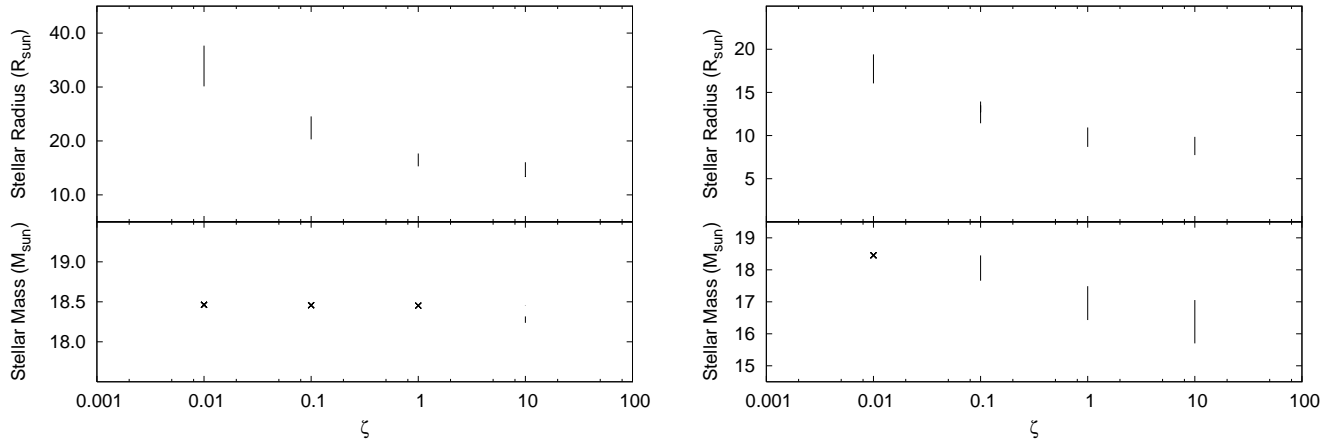


Figure 12. The change in stellar mass/radius with hardness ratio ξ for ULX X-7 in NGC 4559 (left) and the ULX in NGC 5408 (right). We use an inclination of $\cos(i) = 0.5$, a BH mass of $100M_\odot$ and a stellar age of 10Myr. The lines show the range of stellar parameters that fitted with our model at the 90% confidence level. For clarity, we mark with an ‘x’ cases where our model produces a single unique solution.

the NGC 5408 case. We see also an appreciable decrease in stellar mass in this case, but this decrease is still much smaller than the decrease in stellar radius.

In a Roche lobe geometry the shapes of the lobes is determined by the mass ratio of the two components, and the scale of the system is set by their separation. In our model we determine the scale by setting the volume radius of the secondary Roche lobe to be equal to the undistorted radius of the donor star. The results of Figure 12 can therefore be understood as follows. A harder incident X-ray spectrum leads to an accretion disk which is more luminous at optical wavelengths. If the disk in our model is hotter, then to keep it consistent with the observation it must be smaller, so the scale of the Roche lobes must be decreased. Our calculations therefore result in a smaller fitted stellar radius. Since the mass ratio affects only the shape of the Roche lobes, the size of the disk is only weakly dependent on stellar mass, and so varying the hardness ratio will tend to have little effect on this parameter.

In both ULXs, the changes in stellar parameters are smaller than might be expected, given the significant variation in disk luminosity with hardness ratio shown in figure 6 of Copperwheat et al. (2005). This is because that figure did not include the stellar component. Changing the mass ratio results in a different determination of the stellar radius, but changing this parameter results in a change in the luminosity of both the star and the disk. The radius therefore does not need to be changed by much to have a large effect on the overall luminosity.

Through examination of the X-ray data, we have found ξ to vary from ~ 0.1 to ~ 1 in the NGC 4559 ULX. We have assumed this to be a physically appropriate hardness ratio range for all the ULXs in our sample, and have used $\xi = 0.1$ for all the model fits in this paper. Figure 12 indicates that the general findings in this paper will not be invalidated if the X-ray spectrum in these systems is harder than we have assumed. We see that increasing the X-ray hardness to $\xi = 1$ causes no change in the stellar mass in one case and a decrease of $\sim 1M_\odot$ in the other. We see also a decrease in the stellar radius of $2 - 5R_\odot$ as ξ is increased from 0.1

to 1. We conclude therefore that, if the X-ray spectrum is harder, our determinations of the spectral type of the donors are still valid but they may be somewhat smaller and less evolved than our results suggest.

4.6.4 Perturbation of the donor as a result of mass transfer

A key distinguishing feature between the IMBH evolutionary scenarios is the epoch at which the steady mass transfer began. There are two possibilities: (a) we observe the system where mass transfer has not yet significantly affected the state of the star, and so the models we use are a fair description of the donor; (b) we observe it after the mass transfer has already significantly altered the state of the star and a binary evolution code is required for proper modelling.

We note that even in cases when a binary evolution code should be used the results we present here are not initially invalidated. Our method is to determine the star which, in the presence of the intense X-ray radiation field produced by the ULX, will have the appearance of the observed donor, as it exists at the current epoch. Therefore, assuming our model assumptions (such as the assumption that the star is in thermal equilibrium) are correct, the masses and radii will be accurate, since these parameters depend on the current physical state of the star, not its history. Conversely, the parameters we have determined such as the stellar age and ZAMS mass will be inaccurate if the star has lost a significant amount of its mass through Roche lobe overflow.

A binary stellar evolutionary code is necessary when studying a ULX in which the mass transfer has endured long enough for the appearance of the donor to be significantly modified. It is unclear as to how long it takes for a star to deviate in characteristics from the single star evolutionary tracks when it is undergoing mass loss at the rates we have inferred. The mass loss can be assumed to have little affect on very massive stars ($\sim 40M_\odot$ and above) since over the course of their short lives they will transfer only a small percentage of their mass onto the BH through Roche lobe overflow. On the other hand, it has been shown that

low mass stars ($\simeq 1M_{\odot}$) deviate from single star models very rapidly when undergoing phases of high mass transfer (Schenker et al. 2002).

It is reasonable to expect that a star that has transferred, say, 50% of its mass onto the BH through Roche lobe overflow will be significantly perturbed. When we examine the accumulated mass loss for star with ZAMS mass $10 - 20M_{\odot}$, we find that to lose 50% takes $\sim 2 - 3$ Myr when an X-ray luminosity of 10^{40} erg s $^{-1}$ is assumed, although this varies depending on the point in the stellar evolution at which the mass transfer begins. This is a short length of time, but our model predicts the length of time in which any star can sustain mass transfer at ULX rates is also short, even when the effect of the mass loss on the star is not considered. Massive stars can transfer mass at ULX rates from ZAMS, but have intrinsically short (< 10 Myr) lifespans. Lower mass donors only begin to transfer mass at the required rate towards the end of their time on the MS. The maximum duration of the binary as a ULX, assuming a 10^{40} erg s $^{-1}$ X-ray luminosity and a donor ZAMS mass of $10 - 20M_{\odot}$, is around 6 – 8 Myr. Assuming a lower mass transfer rate, as would be expected in ULXs with X-ray luminosities of $\sim 10^{39}$ erg s $^{-1}$, means that the donor takes significantly longer to be perturbed by the mass transfer. We note again that these conclusions are also dependent on the accretion efficiency we have assumed in ULXs being correct.

Note that in this estimation we have assumed the donor is unperturbed at the beginning of the ultraluminous X-ray emitting phase of the binary. Our model suggests that low mass stars can transfer mass at sub-ULX rates in the early part of their lives, assuming they evolve to a semi-detached state shortly after ZAMS. This would mean that the star would already be appreciably perturbed before it began its ULX phase. Similarly, if the star has at some point in its past undergone a phase of extreme mass transfer (such as thermal-timescale mass transfer, as discussed in Section 2.4), then a binary evolution code would almost certainly be necessary. We note also that very high rates of mass transfer are possible even when the driver is nuclear evolution: very massive stars can transfer mass to the BH at a rate of $\sim 10^{-5} M_{\odot}/\text{yr}$ or more, particularly towards the end of their MS life and beyond. This would result in rapid and significant deviation from the single star tracks we have used. Mass transfer at this rate is in excess of what we would expect for the ULXs in our sample, but some very X-ray luminous systems such as the $L_x = \sim 10^{41}$ erg s $^{-1}$ ULX in M82 could have very early type donors in states of extreme mass loss.

We conclude therefore that a binary evolution code may be necessary in some of the sources discussed here, but given that the timescales of the ULX active phase and the timescale for the star to be perturbed by the mass loss are similar, the use of single star tracks is reasonable for this investigation.

5 CONCLUSIONS

We have constructed a model which describes the optical emission from ultra-luminous X-ray sources (ULXs). Our model assumes an X-ray binary nature for ULXs, with the donor star overfilling its Roche lobe. We as-

sume radiative equilibrium and use a radiative transfer formulation to determine the re-radiated thermal emission (Copperwheat et al. 2005). We predict the optical luminosity of the emission from both the irradiated star and a thin accretion disc. We use the mass accretion rate as implied by the observed X-ray luminosity as an additional constraint on the donor star parameters, assuming that the nuclear evolution of the star is the driver for the mass transfer, and hence calculating the mass accretion rate from the rate of increase in radius of the star, compared to the evolution of the Roche lobe.

We have applied our model to optical observations of seven different ULX optical counterparts, and determined the parameters of the donor stars, by fitting the multi-band photometric observations to the optical emission predicted by our model for different sets of stellar parameters. The stellar models were taken from the Geneva stellar evolution tracks of Lejeune & Schaerer (2001). We varied the other parameters in our model, such as binary inclination, position of the star with respect to the observer when the observation was made, BH mass and stellar metallicity, in order to better determine the nature of the donor star.

Previous analysis found that the donor star of ULX are often MS O stars or early-type supergiants. Here we have shown that the donor stars are older and less massive. Their spectral types are generally consistent with MS stars or evolved giants/supergiants of spectral type B or later. They tend to have ages $\sim 10 - 100$ Myr. However the accretion rate necessary to fuel an X-ray luminosity of 10^{40} erg s $^{-1}$ will result in a B-star being completely consumed in 5 – 10 Myr. This implies an upper limit on the duration of the mass transfer. It may be that the capture of the donor by the BH occurred within this period of time, or it could be that binary formed a long time ago but evolved to a semi-detached state within this time. A further possibility is that the donor was originally a much earlier-type, more massive star that has been transferring mass over most of its lifetime, such that it has the appearance of an older and less massive star in the current epoch. The use of binary stellar evolution models will be required to fully explore this possibility.

The ULX in NGC 5204 is an exception to our general findings. Our model cannot provide a good fit with the observation in this case, owing to the constraint we apply on the mass accretion rate. When we remove this constraint the best solution is for an MS O-star in NGC 5204, a more massive donor than has been suggested for this system by other authors. However, our fits suggest a much higher mass accretion rate than would be expected from the X-ray luminosity. A possibility is that this ULX is wind fed, instead of via Roche lobe overflow as we have assumed.

There are a number of systematic effects, which we have discussed. It should be noted that in a number of cases these effects may be greater when we assume a stellar mass BH rather than an IMBH, due to the physics of super-Eddington accretion being uncertain. In stellar mass BH systems the disk geometry may be significantly different from the thin disk approximation we have used, and if there is strong beaming mass transfer may be occurring on thermal timescales. In addition, the effect of radiation pressure may significantly perturb the star, whereas we have shown this effect is small when a more massive BH is used.

We have also discussed the implications for the binary

periods and optical amplitudes, which will be revealed by future observation of these sources. Our model allows us to determine the relative contribution of the star and the disc to the emission. For a less massive BH, the optical/IR emission will be dominated by light from the star. For a more massive BH, the optical/IR emission will be disc dominated. If we assume an irradiating X-ray luminosity of 10^{40} erg s $^{-1}$, the disc will dominate the emission for a BH mass of $> 90M_{\odot}$ if we assume the donor is a typical B-type MS star, and for a BH mass of $> 300M_{\odot}$ if we assume a B supergiant.

In more than half of these systems, we can constrain the mass of the BH based on the optical observations, although the existence of these constraints are dependent on an assumed inclination. If we assume an inclination of $\cos(i) = 0.5$ for the ULX X-1 in NGC 1313, we find the BH has a maximum mass of $\simeq 100M_{\odot}$. If we assume an inclination of $\cos(i) = 0.0$ for the ULXs in NGC 5408 and NGC 4559, we find the BHs in these systems have a maximum mass of $\simeq 110M_{\odot}$ and $\simeq 35M_{\odot}$ respectively. For ULX X-6 in M81, we found a minimum BH mass of $20M_{\odot}$, or a maximum mass of $33M_{\odot}$, depending on the inclination. A temporal optical study of this source could determine with some accuracy the spectral type of the donor, the inclination and the BH mass, so we conclude that this source in particular is an excellent target for further observations with the aim of positively discriminating between stellar mass BH and IMBH scenarios.

ACKNOWLEDGEMENTS

We would like to thank the referee for his/her detailed comments which have led to a number of significant improvements to this paper.

REFERENCES

Allen C. W., 1973, *Astrophysical Quantities*. (London: University of London, Athlone Press)

Begelman M. C., 2002, ApJL, 568, L97

Blecha L., Ivanova N., Kalogera V., Belczynski K., Fregeau J., Rasio F., 2006, ApJ, 642, 427

Bohlin R. C., Savage B. D., Drake J. F., 1978, ApJ, 224, 132

Colbert E. J. M., Mushotzky R. F., 1999, ApJ, 519, 89

Copperwheat C., Cropper M., Soria R., Wu K., 2005, MNRAS, 362, 79

Cropper M., Soria R., Mushotzky R. F., Wu K., Markwardt C. B., Pakull M., 2004, MNRAS, 349, 39

D'Antona F., Mazzitelli I., Ritter H., 1989, A&A, 225, 391

Dewangan G. C., Griffiths R. E., Rao A. R., 2006, ApJL, 641, L125

Done C., Kubota A., 2005, (astro-ph/0511030)

Ebisawa K., Źycki P., Kubota A., Mizuno T., Watarai K.-y., 2003, ApJ, 597, 780

Eggleton P. P., 1983, ApJ, 268, 368

Eldridge J. J., Vink J. S., 2006, A&A, 452, 295

Fabbiano G., 2004, RevMexAA (Serie de Conferencias), 20, 46

Fabbiano G., White N. E., 2003, in *Compact Stellar X-ray Sources*, eds., W. Lewin, W., van der Klis, M., (Cambridge, UK: Cambridge Univ. Press) (astro-ph/0307077)

Fabrika S., 2004, Astrophys. Space Phys. Rev., 12, 1

Gilfanov M., Grimm H.-J., Sunyaev R., 2004, NuPhS, 132, 369

Gonçalves A. C., Soria R., 2006, MNRAS in press, (astro-ph/0606273)

Heger A., Fryer C. L., Woosley S. E., Langer N., Hartmann D. H., 2003, ApJ, 591, 288

Hopman C., Portegies Zwart S. F., Alexander T., 2004, ApJL, 604, L101

Howarth I. D., 1997, The Observatory, 117, 335

Kaaret P., Corbel S., Prestwich A. H., Zezas A., 2003, Science, 299, 365

Kaaret P., Ward M. J., Zezas A., 2004, MNRAS, 351, L83

King A. R., 2002, MNRAS, 335, L13

King A. R., Davies M. B., Ward M. J., Fabbiano G., Elvis M., 2001, ApJL, 552, L109

Körding E., Falcke H., Markoff S., 2002, A&A, 382, L13

Kuntz K. D., Gruendl R. A., Chu Y.-H., Chen C.-H. R., Still M., Mukai K., Mushotzky R. F., 2005, ApJL, 620, L31

Lejeune T., Schaerer D., 2001, A&A, 366, 538

Liu J.-F., Bregman J. N., 2005, ApJS, 157, 59

Liu J.-F., Bregman J. N., Miller J., Kaaret P., 2007, ApJL, submitted

Liu J.-F., Bregman J. N., Seitzer P., 2002, ApJL, 580, L31

Liu J.-F., Bregman J. N., Seitzer P., 2004, ApJ, 602, 249

Maeder A., Meynet G., 1994, A&A, 287, 803

Makishima K., Kubota A., Mizuno T., Ohnishi T., Tashiro M., Aruga Y., Asai K., Dotani T., Mitsuda K., Ueda Y., Uno S., Yamaoka K., Ebisawa K., Kohmura Y., Okada K., 2000, ApJ, 535, 632

Miller J. M., Fabbiano G., Miller M. C., Fabian A. C., 2003, ApJL, 585, L37

Miller J. M., Fabian A. C., Miller M. C., 2004, ApJ, 607, 931

Mucciaelli P., Zampieri L., Falomo R., Turolla R., Treves A., 2005, ApJL, 633, L101

Pakull M. W., Mirioni L., 2002, in Jansen F. et al., eds, *ESA SP-488, Proc. ESA Symp., New Visions of the X-ray Universe in the XMM-Newton and Chandra Era* (astro-ph/0202488)

Phillips S. N., Podsiadlowski P., 2002, MNRAS, 337, 431

Rappaport S. A., Podsiadlowski P., Pfahl E., 2005, MNRAS, 356, 401

Ritter H., 1988, A&A, 202, 93

Roberts T. P., Warwick R. S., 2000, MNRAS, 315, 98

Roberts T. P., Warwick R. S., Ward M. J., Goad M. R., Jenkins L. P., 2005, MNRAS, 357, 1363

Schenker K., King A. R., Kolb U., Wynn G. A., Zhang Z., 2002, MNRAS, 337, 1105

Socrates A., Davis S. W., 2005, (astro-ph/0511549)

Soria R., Cropper M., Pakull M., Mushotzky R., Wu K., 2005, MNRAS, 356, 12

Soria R., Motch C., Read A. M., Stevens I. R., 2004, A&A, 423, 955

Stobart A.-M., Roberts T. P., Wilms J., 2006, MNRAS, 368, 397

Strohmayer T. E., Mushotzky R. F., 2003, ApJL, 586, L61

Strohmayer T. E., Mushotzky R. F., Winter L., Soria

R., Uttley P., Cropper M., 2007, ApJ in press (astro-ph/0701390)

Swartz D. A., Ghosh K. K., Tennant A. F., Wu K., 2004, ApJS, 154, 519

van Paradijs J., van der Klis M., Augusteijn T., Charles P., Corbet R. H. D., Ilovaisky S., Maraschi L., Motch C., Pakull M., Smale A. P., Treves A., van Amerongen S., 1987, A&A, 184, 201

Wu K., 1997, ASPCS, 121, 283

Wu K., Soria R., Hunstead R. W., Johnston H. M., 2001, MNRAS, 320, 177

Zampieri L., Mucciarelli P., Falomo R., Kaaret P., Di Stefano R., Turolla R., Chieregato M., Treves A., 2004, ApJ, 603, 523